AD NUMBER
AD351001
CLASSIFICATION CHANGES
TO: **UNCLASSIFIED**
FROM: **CONFIDENTIAL**
LIMITATION CHANGES
TO: **Approved for public release; distribution is unlimited.**
FROM: **Distribution authorized to U.S. Gov't. agencies and their contractors; Administrative/Operational Use; JUN 1964. Other requests shall be referred to Air Force Arnold Engineering Development Center, Arnold AFB, TN.**
AUTHORITY
10 May 1965 per affdl(fdfr) ltr dtd 23 jun 1965; 20 dec 1974 per tab 74-26

AEDC-TDR-64-120

DECLASSIFIED / UNCLASSIFIED

[redacted]

ARCHIVE COPY
DO NOT LOAN

ARO, INC.
DOCUMENT CONTROL
NO 1G-503-343
COPY IX OF 42
SERIES A PAGES 50

(TITLE UNCLASSIFIED)

AERODYNAMIC CHARACTERISTICS OF VARIOUS TYPES OF FULL SCALE PARACHUTES AT MACH NUMBERS FROM 1.8 TO 3.0

Per TAB 74-26
Dtd 20 Dec, 1974

Approved for public release; distribution unlimited.

By

J. F. Lowry

Propulsion Wind Tunnel Facility

ARO, Inc.

TECHNICAL DOCUMENTARY REPORT NO. AEDC-TDR-64-120

CLASSIFICATION CANCELLED (CHANGED TO ....)
BY AUTHORITY OF AEDL(FDFR) Letter
dtd 11 May 65 Official authorized to change
BY E Boyd
Name and Position of Individual
JUN 23 1965
Date

June 1964

AFSC Program Area 921A

(Prepared under Contract No. AF 40(600)-1000 by ARO, Inc., contract operator of AEDC, Arnold Air Force Station, Tenn.)

ARNOLD ENGINEERING DEVELOPMENT CENTER

AIR FORCE SYSTEMS COMMAND

UNITED STATES AIR FORCE

[redacted]

DECLASSIFIED / UNCLASSIFIED

[redacted]

NOTICES

Qualified requesters may obtain copies of this report from DDC, Cameron Station, Alexandria, Va. Orders will be expedited if placed through the librarian or other staff member designated to request and receive documents from DDC.

When Government drawings, specifications or other data are used for any purpose other than in connection with a definitely related Government procurement operation, the United States Government thereby incurs no responsibility nor any obligation whatsoever; and the fact that the Government may have formulated, furnished, or in any way supplied the said drawings, specifications, or other data, is not to be regarded by implication or otherwise as in any manner licensing the holder or any other person or corporation, or conveying any rights or permission to manufacture, use, or sell any patented invention that may in any way be related thereto.

This document contains information affecting the national defense of the United States within the meaning of the Espionage Laws (Title 18, U.S.C., sections 793 and 794) the transmission or revelation of which in any manner to an unauthorized person is prohibited by law.

This docum... ...ic release

PER TAB 74-26
Dtd 20 Dec, 1974

ERRATA

AEDC-TDR-64-120, June 1964

AERODYNAMIC CHARACTERISTICS OF VARIOUS TYPES OF FULL SCALE PARACHUTES AT MACH NUMBERS FROM 1.8 TO 3.0

J. R. Lowry, ARO, Inc.

Arnold Engineering Development Center
Air Force Systems Command
Arnold Air Force Station, Tennessee

Please note the following revisions to Figs. 25 and 26 on page 40:

Legends are	M_∞
○	2.0
□	2.2
△	2.6

Legends should be	M_∞
○	2.2
□	2.6
△	2.0

(Title Unclassified)
AERODYNAMIC CHARACTERISTICS OF VARIOUS TYPES OF FULL SCALE PARACHUTES AT MACH NUMBERS FROM 1.8 TO 3.0

By

J. F. Lowry

Propulsion Wind Tunnel Facility

ARO, Inc.

a subsidiary of Sverdrup and Parcel, Inc.

June 1964

ARO Project No. PS0434

(This abstract is UNCLASSIFIED.)

ABSTRACT

As an extension of studies previously completed in the von Kármán Gas Dynamics Facility, a test was conducted in the Propulsion Wind Tunnel, Supersonic (16S), to determine the effect of Mach number on the drag, stability, and inflation characteristics of four types of parachutes. The parachute characteristics were investigated at Mach numbers from 1.8 to 3.0 at pressure altitudes from 75,000 to 104,000 ft. Hyperflo parachutes were tested with 14 different roof configurations, hemisflo and conical parachutes with two different shroud line lengths and a butted skirt. A supersonic-guide-surface parachute was tested at various parachute-centerbody separation distances.

Data obtained indicate that for all parachute configurations, drag decreased with increasing Mach number. For the hyperflo parachutes, it was determined that the higher porosity parachutes tended to be underinflated, resulting in a much lower drag coefficient than the lower porosity parachutes. The hemisflo and conical parachutes had good stability and inflation characteristics. The supersonic-guide-surface parachute displayed good inflation characteristics at all conditions and generally increased in stability as the separation distance between the parachute and the centerbody was increased.

PUBLICATION REVIEW

This report has been reviewed and publication is approved.

Frank F. Marvin
Lt Col, USAF
AF Representative, PWT
DCS/Test

Jean A. Jack
Colonel, USAF
DCS/Test

CONTENTS

TABLES

ILLUSTRATIONS

NOMENCLATURE

C_DA	Parachute drag parameter, $\frac{drag}{q_\infty}$, ft^2
C_{D_o}	Parachute drag coefficient, $\frac{drag}{q_\infty S_o}$
D	Model centerbody diameter, 1.47 ft
d_R	Reefed inlet diameter of hemisflo and conical parachutes, ft
M_∞	Free-stream Mach number
q_∞	Free-stream dynamic pressure, psfa
S_o	Parachute surface area, ft^2
X	Distance from aft end of model centerbody to parachute inlet, ft

1.0 INTRODUCTION

At the request of the Research and Technology Division (RTD) of the Air Force Systems Command (AFSC), a test was conducted in the Propulsion Wind Tunnel, Supersonic (16S), of the Propulsion Wind Tunnel Facility (PWT) at the Arnold Engineering Development Center (AEDC), AFSC, to determine the effect of Mach number on the drag, stability, and inflation characteristics of various parachutes. This investigation was conducted during the period from March 16 to April 3, 1964, for the Air Force Flight Dynamics Laboratory, (AFFDL), AFSC, Wright-Patterson Air Force Base, Ohio.

The parachutes investigated during this test were fabric models of the hemisflo, hyperflo, and conical families of parachutes with the exception of the supersonic-guide-surface parachute which had an aluminum cone suspended within the shroud lines of the fabric parachute.

This investigation was primarily an extension of the studies conducted in the von Karman Gas Dynamics Facility on several small-scale prototype aerodynamic decelerators. The prototype studies which are reported in Refs. 1 through 4 resulted in the configurations that were investigated during the test in 16S.

The hyperflo, hemisflo, conical, and supersonic-guide-surface parachute configurations were tested at Mach numbers from 1.8 to 3.0 at pressure altitudes from 75,000 to 104,000 ft. Various canopy porosities for the hyperflo parachutes were investigated at these Mach numbers. The hemisflo parachute characteristics were studied with two different shroud line lengths at reefed diameters of 1.5 and 2 ft and with a butted skirt. The effect of separation distance between the model centerbody and the parachute, as well as Mach number, was investigated for the supersonic-guide-surface configuration. Dynamic drag during deployment, steady-state drag after stabilization, and motion pictures of the parachutes were recorded for each of the configurations.

It should be noted that the roof failures experienced by the parachutes tested were not necessarily a deficiency in the parachute material or construction but a result of the testing technique. These parachutes were required to withstand constant loads at elevated Mach numbers for long durations of time, which resulted in failure caused by material fatigue.

Manuscript received May 1964.

2.0 APPARATUS

2.1 TEST FACILITY

Tunnel 16S is a closed-circuit, continuous flow tunnel with a test section 16 ft in cross section, capable of operating at supersonic Mach numbers from 1.65 to 3.2. The tunnel was designed for a stagnation pressure range from 100 to 2000 psfa and air temperatures up to 650°F. Tunnel humidity is controlled by removing tunnel air and supplying conditioned make-up air from an atmospheric dryer. A more complete description of the facility and its operating characteristics is contained in Ref. 5. The location and installation of the model centerbody in the tunnel are shown in Figs. 1 and 2.

2.2 TEST ARTICLE

2.2.1 Model Centerbody and Deployment System

The parachutes tested during this investigation were deployed from a strut-mounted centerbody. Dimensions of the centerbody are presented in Fig. 3. This centerbody contained a swivel that alleviated twisting of the shroud lines. A strain-gage load cell was used to measure parachute drag. The hyperflo, hemisflo, and conical parachutes were packed into the aft end of the model centerbody on a compressed spring and released by means of an explosive charge which ejected the parachute pack from the centerbody into the airstream. The supersonic-guide-surface parachute was attached by a cable-pulley system through the centerbody to a winch outside the tunnel shell. The pulley system, which also contained the strain-gage drag link, allowed the decelerator to be translated the length of the test section.

2.2.2 Parachutes

The parachutes tested were of four general types: hyperflo, hemisflo, conical, and supersonic-guide-surface. General construction details for these parachutes are given in Table 1 and Figs. 4 through 17.

2.2.2.1 Hyperflo Parachutes

The hyperflo parachutes were constructed with various porosities from 7.4 to 16.9 percent using two design concepts. Configurations H-1, H-2, H-3, and H-8 through H-14 as seen in Figs. 4 and 6 through 12 were designed in the shape of a truncated cone. Configurations H-4 through H-7

were constructed in the shape that the truncated cone design assumes when it is in a fully aerodynamically inflated condition. Details of the shaped hyperflo parachute are shown in Fig. 5. Porosities of these hyperflo parachutes were varied by constructing them of perlon, nylon, and HT-1 material of various weaves and porosities as indicated in Table 1.

2.2.2.2 Hemisflo and Conical Parachutes

The hemisflo and conical parachutes were constructed of 2-in-wide nylon ribbons. Configurations R-1, R-2, and R-3 were 10-ft-diam hemisflo parachutes with 14-percent porosity. Configurations R-1 and R-3 had shroud lines 240 in. in length, and configuration R-2 had shroud lines 120 in. in length. Details of configurations R-1 and R-2 are shown in Fig. 13. Configuration R-3 also had a butted ribbon skirt and is shown in Fig. 14. Configurations R-2 and R-5 were 10-ft-diam conical parachutes of 14-percent porosity. Configuration R-4 had shroud lines 240 in. in length, and configuration R-5 had shroud lines 120 in. in length. Details of these parachutes are given in Fig. 15. Configuration R-6 was a cluster of two 6-ft-diam conical parachutes with a porosity of 25 percent and using shroud lines 75.5 in. in length. Details of this configuration are shown in Fig. 16.

2.2.2.3 Supersonic-Guide-Surface Parachute

The supersonic-guide-surface parachute, configuration A-1, has a 34-deg half-angle cone suspended by nylon lines at the inlet of the nylon parachute. The nylon parachute has a 48-in. maximum diameter which reduces to a 30.5-in.-diam open nozzle at the aft section of the parachute. The cone is constructed of foam plastic laminated between two concentric aluminum cones, with the inside cone completely filled with the foam plastic. Details of configuration A-1 are shown in Fig. 17.

3.0 PROCEDURE

Before the beginning of tunnel operation during the testing of the hyperflo, hemisflo, and conical configurations, the parachute was packed into the aft end of the centerbody. After tunnel conditions were established, the parachute was deployed by a compressed spring. Motion pictures and dynamic drag data were obtained during each deployment. Steady-state drag readings were recorded after the parachute deployment had been completed. Tunnel conditions were then changed with the parachute still deployed, and steady-state drag data were obtained at all subsequent desired test conditions.

Fourteen hyperflo-type parachutes with varying roof porosities were tested. Two hemisflo and two conical configurations were investigated for varying shroud line lengths. A cluster of two conical parachutes was also tested. The hyperflo parachutes were positioned approximately eight centerbody diameters downstream of the model centerbody and the hemisflo and conical parachutes approximately fifteen centerbody diameters.

After test conditions were established, the supersonic-guide-surface parachute was deployed and translated the length of the test section. Dynamic and steady-state drag data were obtained for various centerbody-parachute separation distances.

All parachute configurations were investigated at Mach numbers in the range from 1.8 to 3.0. Dynamic pressure was maintained nominally at 120 psfa for all except configurations H-11 and H-12, for which the dynamic pressure was varied to maintain a pressure altitude of 75,000 ft. The dynamic pressure of 120 psfa resulted in pressure altitudes from 82,000 to 104,000 ft over the Mach number range investigated. The model centerbody was maintained at zero angle of attack for the entire test. (See Tables 2, 3, and 4 for test conditions.)

4.0 RESULTS AND DISCUSSION

4.1 DEPLOYMENT LOADS

During deployment of the parachutes, it was found that the shock load, when the deployment bag reached the end of the shroud lines, and the opening loads varied with each deployment. Shown in Fig. 18 are two typical drag traces, one with an appreciable opening load and one with a negligible opening load. Shock and opening loads were found to vary between 200 and 2500 lb for all the deployments, although large shock and opening loads did not necessarily occur during the same deployment. It is believed that the shock and opening loads encountered during these tests were a function of the parachute packing procedures and the particular deployment system used for each parachute.

4.2 HYPERFLO PARACHUTES

As indicated in Figs. 19 and 20, the drag coefficient and parachute drag parameter for the hyperflo parachutes were found to decrease with increasing Mach number. For configuration H-12, which was the only

configuration tested over the complete Mach number range, the drag coefficient decreased approximately 25 percent. Although none of the other parachutes were tested over the complete Mach number range, the data taken follow the same trend as that for configuration H-12.

The drag coefficient for the fully inflated hyperflo parachutes was found to range from 0.18 to 0.34. For the underinflated parachutes and the ones with torn roofs, the drag coefficient varied from approximately 0.05 to 0.10. Configurations H-4, H-5, and H-6 were shaped parachutes with porosities of 15.2, 16.9, and 13.5 percent, respectively, and were observed to be underinflated. Configuration H-7 was a shaped hyperflo sprayed with a plastic coating to reduce its total porosity to nine percent. This lower porosity parachute inflated properly and had a much higher drag coefficient and drag parameter than the higher porosity shaped configuration. The drag coefficient and drag parameter measured for each configuration are presented in Table 2.

Stability and inflation characteristics of the hyperflo parachutes were visually studied from motion pictures which indicated that there was no appreciable effect of Mach number on the stability or inflation of the parachutes. However, some of the more porous parachutes (H-4, H-5, and H-6) were underinflated and tended to be more stable than the less porous, fully inflated parachutes. The low porosity parachutes also tended to become underinflated and more stable when the roofs began to fail, effectively increasing the porosity. Typical pictures taken during testing of a number of these parachutes are presented in Fig. 21, which shows the underinflation of these higher porosity parachutes. Stability and inflation characteristics and the test conditions for each configuration tested are presented in Table 2.

4.3 HEMISFLO AND CONICAL PARACHUTES

The results of tests conducted on the hemisflo and conical parachutes are presented in Figs. 22 and 23 and Table 3. For all the hemisflo and conical configurations, the drag coefficient was found to vary between 0.035 and 0.060, except configuration R-6 (conical cluster) which ranged from 0.10 to 0.17. The drag coefficient and drag parameter for all configurations decreased with increasing Mach number. It was found that reducing the shroud line length from 240 in. to 120 in. for the conical parachutes reduced the drag coefficient approximately eight percent. The drag coefficient for the hemisflo parachute with the addition of a butted skirt at a reefing diameter of 2.0 ft was less than that of an open skirt at a reefing diameter of 1.5 ft. All of the hemisflo and conical configurations

which were investigated had fair to good stability and good inflation except configuration R-3 which was rigged incorrectly. Figure 24 shows typical pictures taken during testing that illustrate the inflation characteristics of the reefed hemisflo and conical parachutes.

4.4 SUPERSONIC-GUIDE-SURFACE PARACHUTE

Test results for the supersonic-guide-surface parachute (configuration A-1) shown in Fig. 25 and Table 4 indicate that maximum drag coefficient occurs at a greater centerbody-parachute separation distance as Mach number is increased. It was also found that the level of maximum drag coefficient decreases with increasing Mach number at a constant dynamic pressure, as was found for the other types of parachutes.

As shown in Fig. 26, the stability of configuration A-1 generally increases as centerbody-parachute separation distance increases. However, at a Mach number of 2.0 and X/D of 14, the parachute became more unstable than at any other condition. This could have been caused by shocks originating from the strut and centerbody being reflected from the tunnel walls. There appeared to be no effect of Mach number on the stability of the parachute. Figure 27 represents pictures taken of configuration A-1 during testing and illustrates the inflation characteristics and cone positioning of this parachute.

5.0 CONCLUSIONS

Tests conducted to investigate the drag, stability, and inflation characteristics of several types of parachutes resulted in the following conclusions:

1. The drag coefficient and drag parameter decreased with increasing Mach number for all configurations tested.
2. Stability was essentially constant with varying Mach number for all configurations tested.
3. The higher porosity hyperflo parachutes tended to be underinflated and had a much lower drag coefficient than the lower porosity parachutes.
4. For the range of these tests, the hemisflo and conical parachutes had good stability and good inflation characteristics.
5. The maximum value of the drag coefficient and the stability of the supersonic-guide-surface parachute were dependent on the separation distance between the parachute and centerbody.

REFERENCES

1. Morgan, L. A. "Wind Tunnel Investigation of Flexible Parachute Models at Supersonic Speeds." AEDC-TN-61-176, January 1962.

2. Deitering, J. S. "Investigation of Flexible Parachute Model Characteristics at Mach Numbers from 1.5 to 6." AEDC-TDR-62-185, October 1962. (CONFIDENTIAL)

3. Deitering, J. S. "Performance of Flexible Parachute Models at Mach Numbers from 1.5 to 4." AEDC-TDR-62-234, December 1962. (CONFIDENTIAL)

4. Deitering, J. S. "Performance of Flexible Aerodynamic Decelerators at Mach Numbers from 1.5 to 6." AEDC-TDR-63-119, July 1963. (CONFIDENTIAL)

5. Test Facilities Handbook, (5th Edition). "Propulsion Wind Tunnel Facility, Vol. 3." Arnold Engineering Development Center, July 1963.

TABLE 1

PARACHUTE MATERIAL DETAILS

Configuration	Type	Total Porosity, Percent	Description
H-1	Hyperflo	13.3	Perlon mesh roof material with a 64/in. x 68/in. thread count and nylon skirt material.
H-2	Hyperflo	9.4	HT-1 mesh roof material with a thread count of 15/in. (4 strands per thread) x 22/in. (3 strands per thread) and nylon skirt material.
H-3	Hyperflo	11.4	HT-1 mesh roof material with a thread count of 18/in. (3 strands per thread) x 20/in. (3 strands per thread) and nylon skirt material.
H-4	Hyperflo	15.2	Perlon mesh roof material with a thread count of 64/in. x 68/in. and nylon skirt material.
H-5	Hyperflo	16.9	HT-1 mesh roof material with a thread count of 18/in. (3 strands per thread) x 20/in. (3 strands per thread) and nylon skirt material.
H-6	Hyperflo	13.5	HT-1 mesh roof material with a thread count of 15/in. (4 strands per thread) x 22/in. (3 strands per thread) and nylon skirt material.
H-7	Hyperflo	9.0	HT-1 mesh roof material having a 24-percent porosity with a 11-in.-radius circle from center of parachute coated with silicone to give a porosity of 10.9 percent for the circle. HT-1 skirt material.
H-8	Hyperflo	13.0	Perlon mesh roof material with a thread count of 64/in. x 64/in. and HT-1 skirt material.
H-9	Hyperflo	7.5	Nylon ribbon roof material and HT-1 skirt material.
H-10	Hyperflo	14.5	Type 304 stainless steel mesh disc with a strand count of 64/in. x 64/in. and nylon skirt material.

TABLE 1 (Concluded)

Configuration	Type	Total Porosity, Percent	Description
H-11	Hyperflo	14.6	Nylon ribbon roof material and nylon skirt material.
H-12	Hyperflo	14.3	Perlon mesh roof material with a thread count of 64/in. x 64/in. and nylon skirt material.
H-13	Hyperflo	13.7	Nylon ribbon roof material and HT-1 skirt material.
H-14	Hyperflo	14.0	Nylon ribbon roof material and HT-1 skirt material.
R-1	Hemisflo	14.0	10-ft-diam parachute constructed of 2-in.-wide nylon ribbons with 240-in. nylon suspension lines.
R-2	Hemisflo	14.0	10-ft-diam parachute constructed of 2-in.-wide nylon ribbons and using pocket bands to aid inflation. This parachute has 120-in. nylon suspension lines.
R-3	Hemisflo	14.0	10-ft-diam parachute constructed of 2-in.-wide nylon ribbons with a butted ribbon skirt. This parachute has 240-in. nylon suspension lines.
R-4	Conical	14.0	10-ft-diam parachute constructed of 2-in.-wide nylon ribbons with 240-in. nylon suspension lines.
R-5	Conical	14.0	10-ft-diam parachute constructed of 2-in.-wide nylon ribbons and using pocket bands to aid inflation. This parachute has 120-in. nylon suspension lines.
R-6	Conical	25.0	Two 6-ft-diam parachutes attached at the confluence point. These parachutes are constructed of 2-in.-wide nylon ribbons and have 75.5-in. nylon suspension lines.
A-1	Supersonic-Guide-Surface		34-deg half-angle cone made of foam plastic between two concentric aluminum cones. The inner cone was completely filled with the plastic foam. This cone was suspended at the inlet by nylon suspension lines. Fabric parachute was nylon.

TABLE 2

HYPERFLO PARACHUTE TEST CONDITIONS AND RESULTS

Config.	M_∞	q_∞	C_DA	C_{D_o}	Observations
H-1	2.60	120.4	2.78	0.222	Fair stability, good inflation with heavy squiding, suspension line failed.
H-2	2.60	120.6	3.00	0.239	Good stability, good inflation with slight squiding, suspension line failed.
H-3	2.50	119.8	2.69	0.212	Poor stability, good inflation with heavy squiding.
	2.80	120.0	1.06	0.085	Poor stability, poor inflation, roof failing.
	3.00	121.0	1.80	0.140	Poor stability, poor inflation, roof failing.
H-4	2.19	121.5	0.74	0.059	Good stability, poor inflation.
	2.00	120.2	0.85	0.067	Good stability, poor inflation.
	1.80	120.0	0.96	0.077	Good stability, poor inflation, roof failing.
H-5	2.60	120.3	1.18	0.094	Good stability, poor inflation.
	2.80	120.0	0.99	0.078	Fair stability, poor inflation, roof failing.
H-6	2.49	119.0	0.88	0.070	Good stability, poor inflation.
	2.73	120.0	0.70	0.056	Good stability, poor inflation, roof failing.
H-7	2.60	120.0	3.19	0.255	Good stability, good inflation.
H-8	2.60	120.0	1.55	0.263	Good stability, good inflation.
	2.80	119.2	1.38	0.236	Good stability, good inflation.
	3.00	117.1	1.22	0.209	Fair stability, good inflation.
H-9	2.61	121.2	3.62	0.339	Poor stability, good inflation.

{ Denotes continuous run.

TABLE 2 (Concluded)

Config.	M_∞	q_∞	C_DA	C_{D_O}	Observations
H-10	2.19	121.6	3.14	0.294	Good stability, good inflation.
	2.01	120.3	3.11	0.290	Good stability, good inflation.
	1.92	114.0	0.93	0.870	Good stability, poor inflation, roof failing.
H-11	2.20	250.1	3.06	0.286	Poor stability, good inflation.
	2.00	207.0	3.15	0.295	Fair stability, good inflation, roof failing.
H-12	2.20	249.1	2.81	0.262	Good stability, good inflation.
	2.00	207.4	2.89	0.270	Good stability, good inflation.
	1.80	167.8	2.91	0.272	Good stability, good inflation.
	2.60	120.1	2.42	0.226	Good stability, good inflation.
	2.80	119.4	2.20	0.206	Good stability, good inflation.
	3.01	119.1	2.12	0.198	Good stability, good inflation.
H-13	2.59	121.5	2.13	0.199	Poor stability, good inflation.
	2.80	120.2	0.80	0.076	Good stability, poor inflation, roof failing.
	3.00	118.6	0.86	0.081	Good stability, poor inflation, roof failing.
H-14	2.60	121.1	1.22	0.212	Poor stability, good inflation, light squiding.
	2.84	119.9	1.04	0.181	Fair stability, good inflation, light squiding.
	3.01	120.8	1.08	0.189	Fair stability, good inflation, light squiding.

{ Denotes continuous run.

TABLE 3

HEMISFLO AND CONICAL PARACHUTE TEST CONDITIONS AND RESULTS

Config.	M_∞	q_∞	C_DA	C_{D_o}	d_R	Observations
R-1	2.20	121.0	4.72	0.0602	1.5	Fair stability, good inflation.
R-2	2.59	121.1	3.83	0.0488	2.0	Good stability, good inflation.
	2.80	119.7	3.30	0.0421	2.0	Good stability, good inflation.
	3.00	117.0	2.92	0.0373	2.0	Good stability, good inflation.
R-3	2.19	121.3	4.11	0.0524	2.0	Poor stability, good inflation, incorrect reefing probable cause of instability.
	1.99	120.4	2.47	0.0315	2.0	Fair stability, poor inflation, shroud lines winding, incorrect reefing probable cause of winding and under-inflation.
	1.80	120.3	2.34	0.0299	2.0	Fair stability, poor inflation, shroud lines winding, incorrect reefing probable cause of winding and under-inflation.
R-4	2.59	121.7	3.41	0.0435	1.5	Good stability, good inflation.
	2.79	120.0	3.11	0.0397	1.5	Good stability, good inflation.
	2.90	117.0	2.37	0.0302	1.5	Good stability, good inflation. Broken shroud line with probable spillage.
R-5	2.59	122.0	3.07	0.0391	1.5	Good stability, good inflation.
	2.79	120.0	2.93	0.0374	1.5	Good stability, good inflation.
	3.00	117.0	2.73	0.0348	1.5	Good stability, good inflation.
R-6	1.80	139.9	9.65	0.1710	6.0	Fair stability, good inflation.
	1.99	121.0	6.23	0.1110	6.0	Fair stability, good inflation.
	2.19	121.4	5.90	0.1050	6.0	Fair stability, good inflation.

{ Denotes continuous run.

TABLE 4

SUPERSONIC-GUIDE-SURFACE PARACHUTE TEST CONDITIONS AND RESULTS

Config.	M_∞	q_∞	C_DA	C_{D_o}	X/D	Observations
A-1	2.20	120.4	9.36	0.747	9.7	Poor stability, good inflation.
	2.20	120.5	9.89	0.787	11.6	Poor stability, good inflation.
	2.20	120.3	9.68	0.771	13.7	Fair stability, good inflation.
	2.20	120.3	9.13	0.726	15.5	Fair stability, good inflation.
	2.20	120.3	9.10	0.724	17.6	Good stability, good inflation.
	2.20	120.5	9.23	0.735	20.0	Fair stability, good inflation.
	2.01	119.9	9.94	0.791	9.7	Poor stability, good inflation.
	2.01	120.1	9.65	0.770	11.6	Poor stability, good inflation.
	2.01	119.9	9.31	0.741	13.7	Fair stability, good inflation.
	2.01	120.0	9.09	0.724	15.5	Good stability, good inflation.
	2.01	120.2	9.29	0.739	17.6	Good stability, good inflation.
	2.01	120.0	9.30	0.740	19.5	Good stability, good inflation.
	2.60	120.1	7.73	0.615	9.7	Poor stability, good inflation.
	2.60	120.0	7.78	0.620	11.6	Poor stability, good inflation.
	2.60	120.5	8.03	0.639	13.7	Fair stability, good inflation.
	2.60	120.2	8.31	0.661	15.5	Good stability, good inflation.
	2.60	120.4	8.30	0.660	17.6	Good stability, good inflation.
	2.60	120.8	7.73	0.614	19.5	Good stability, good inflation.

{ Denotes continuous run.

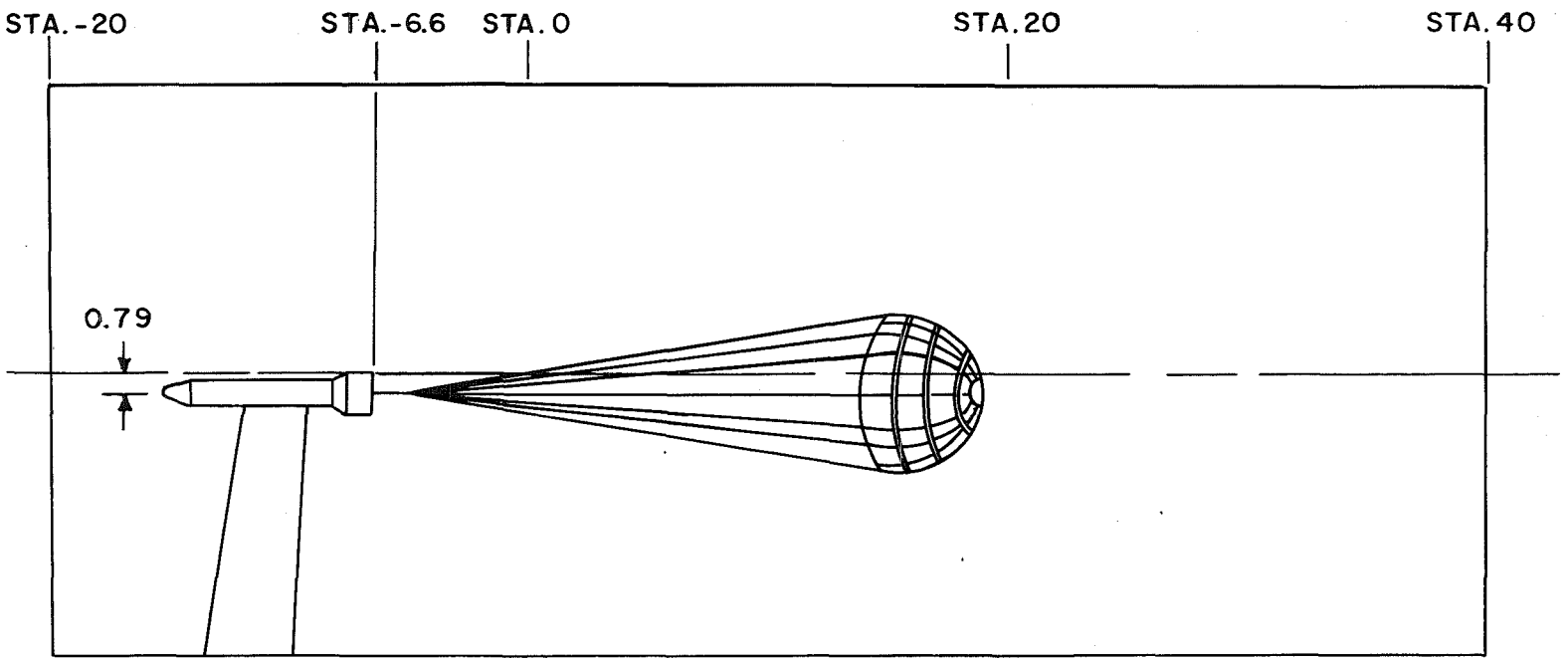

NOTE: ALL STATIONS ARE TUNNEL STATIONS
WITH DIMENSIONS IN FEET

101502

Fig. 1 Location of Model Centerbody in 16S Test Section

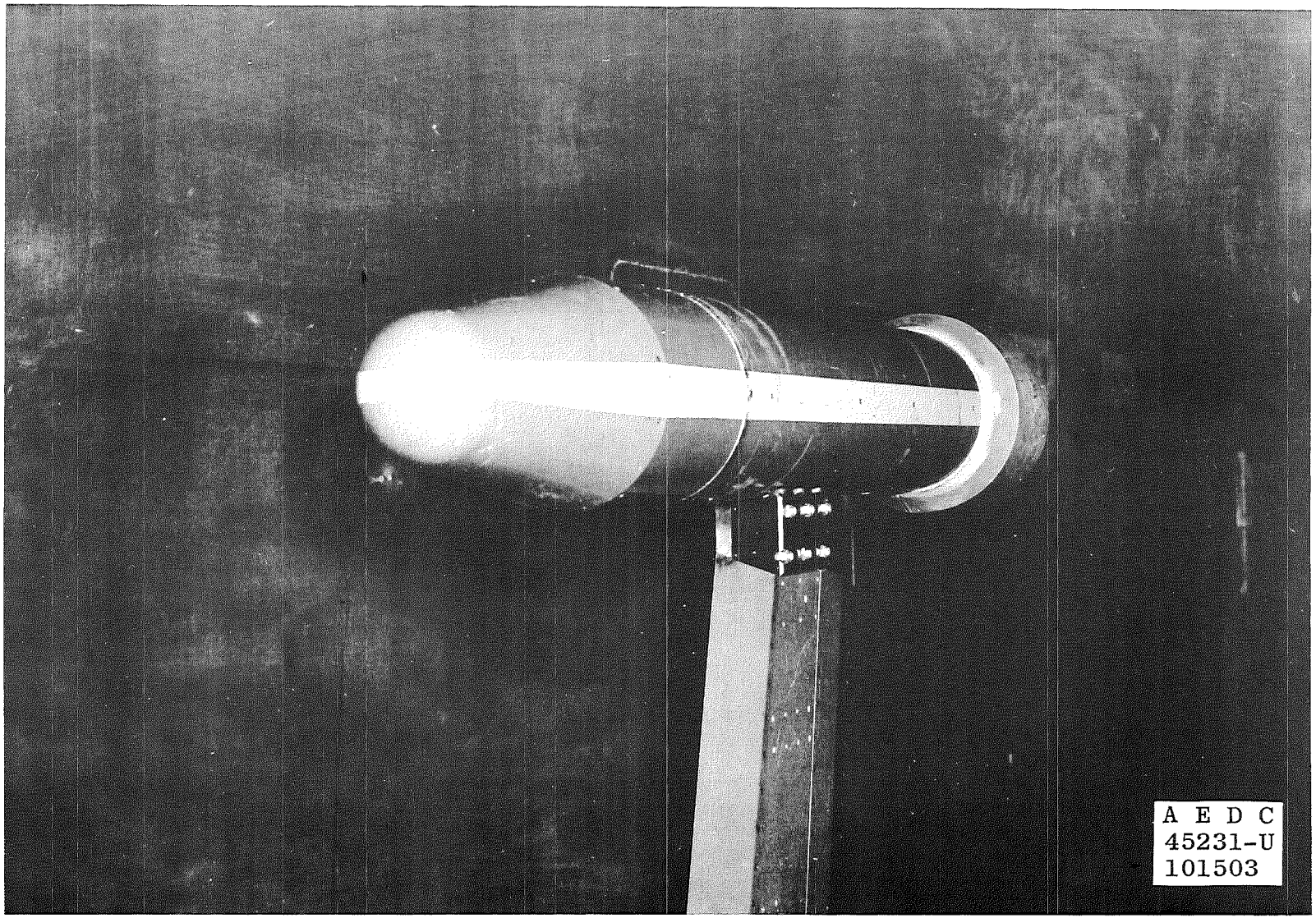

Fig. 2 Installation of Model Centerbody in 16S Test Section

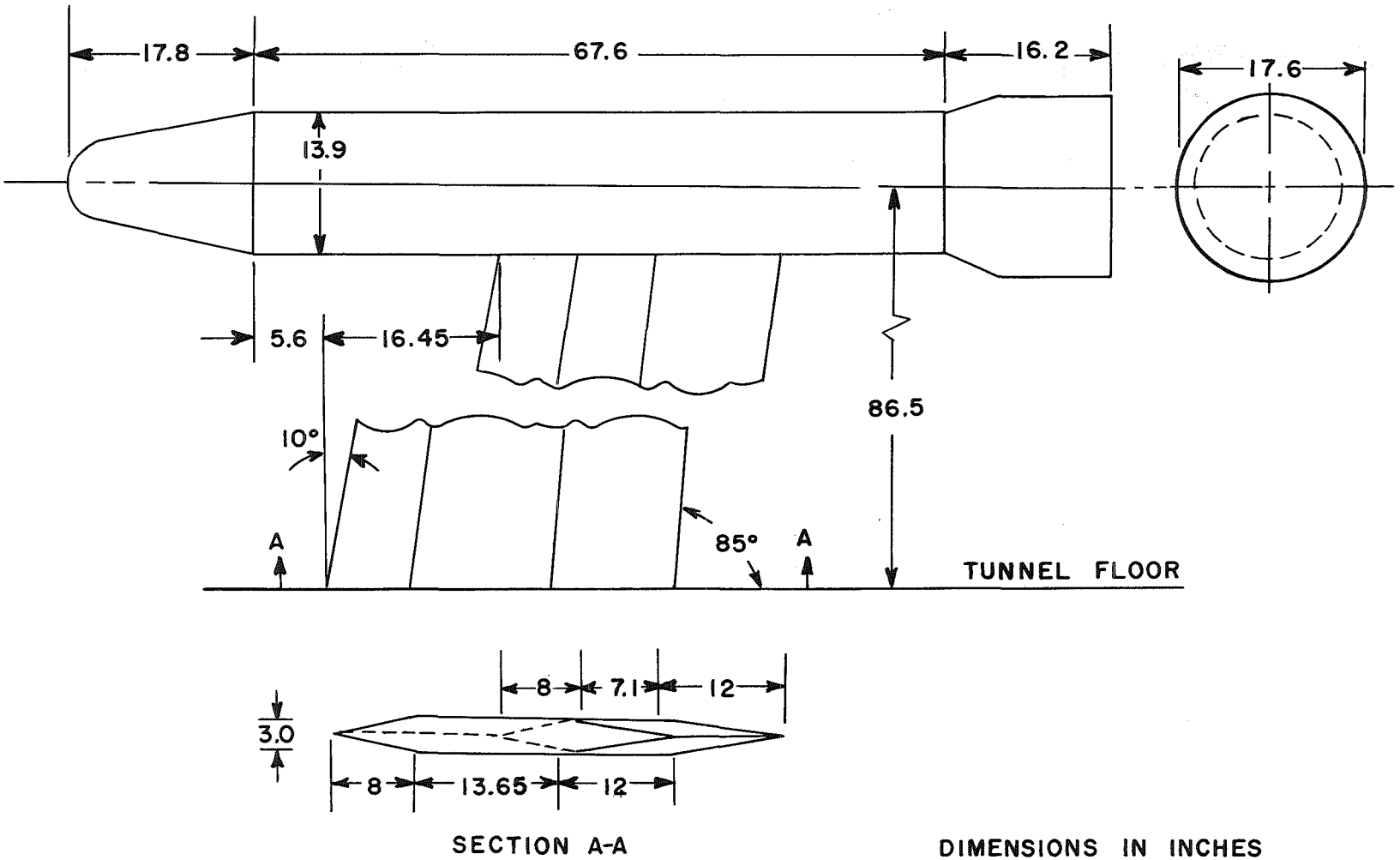

Fig. 3 Model Centerbody Dimensions

AEDC-TDR-64-120

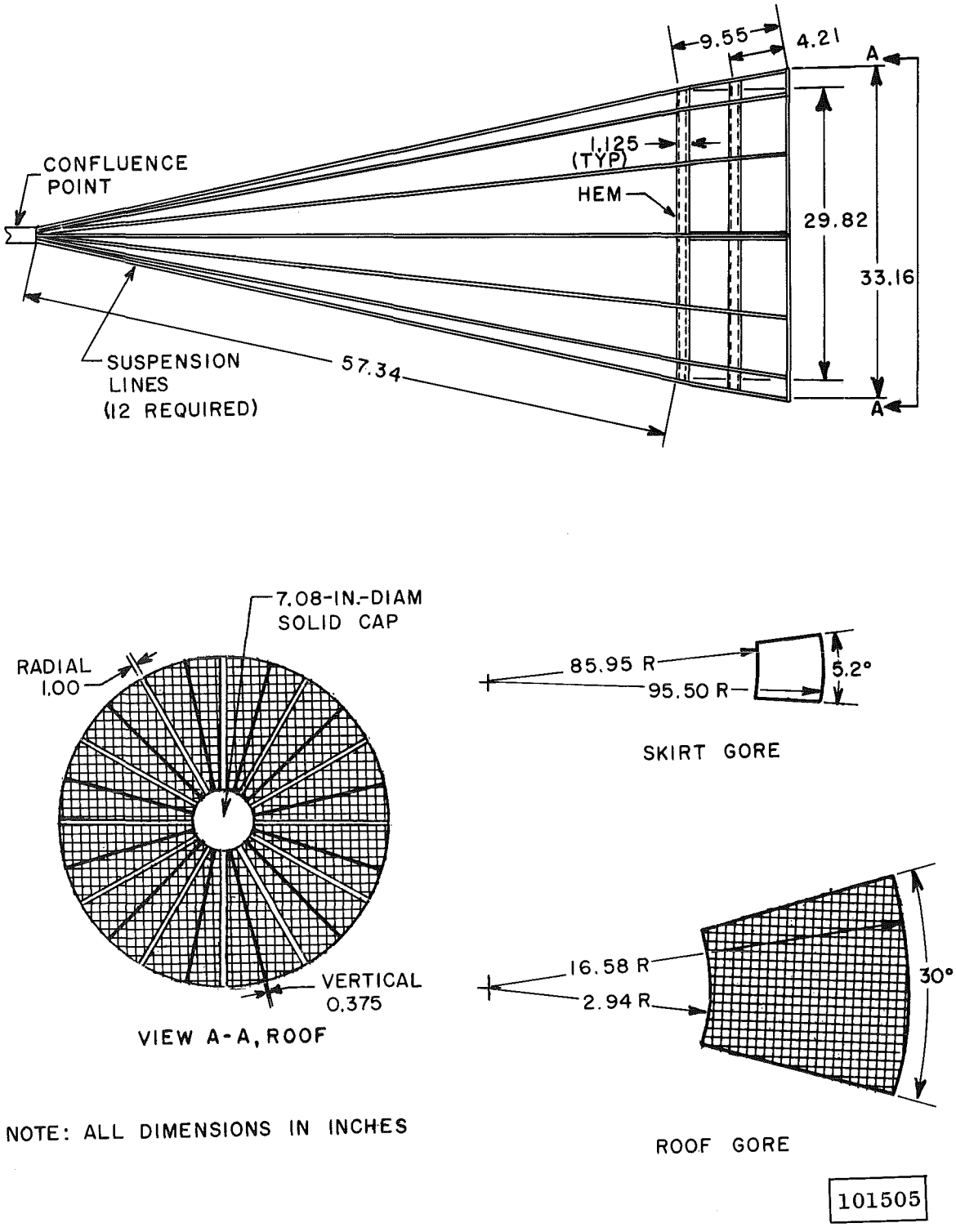

Fig. 4 Hyperflo Parachute Details, Configurations H-1, H-2, and H-3

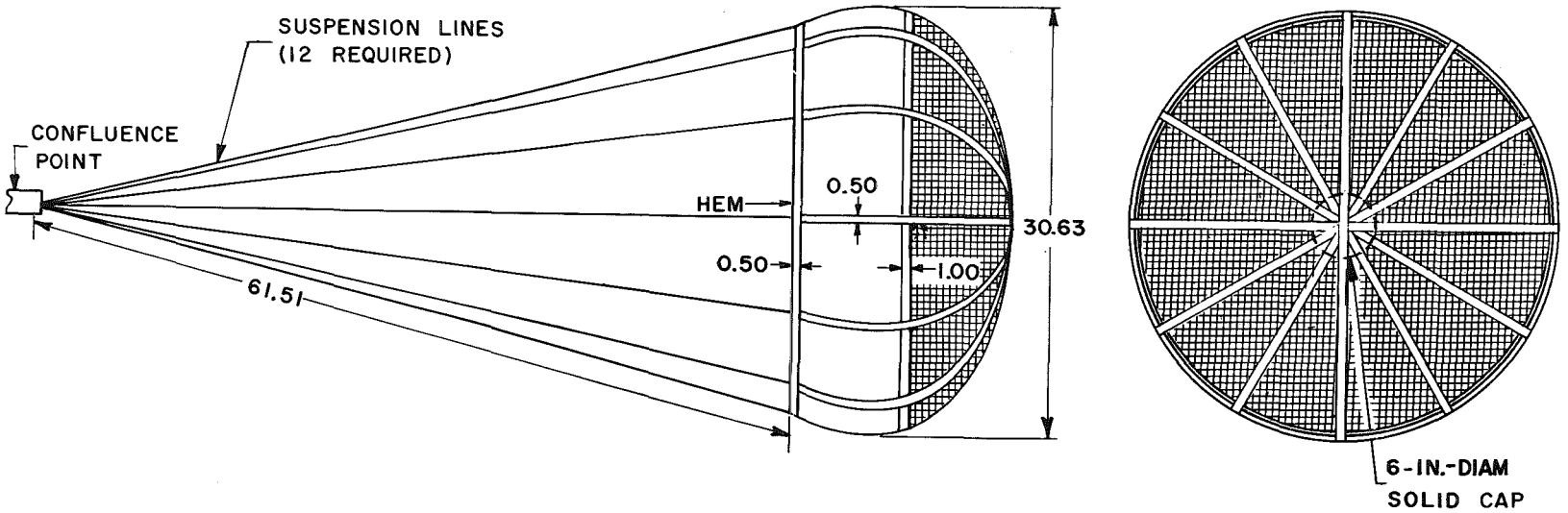

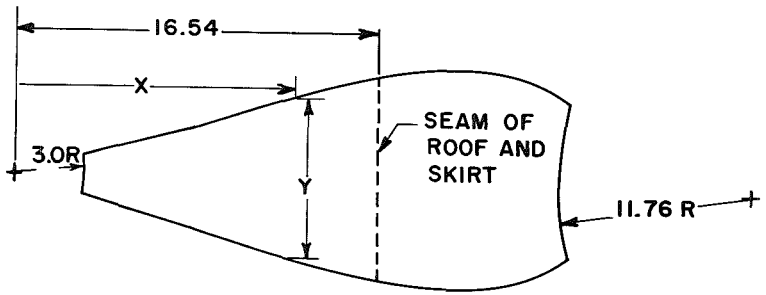

ROOF AND SKIRT GORE

ROOF AND SKIRT GORE COORDINATES

X	Y	X	Y
0.766	0.398	15.315	8.730
1.532	0.858	16.540	9.189
3.063	1.685	16.847	9.281
4.595	2.542	18.378	9.679
6.126	3.400	19.910	9.802
7.658	4.288	20.032	9.832
9.189	5.207	21.441	9.648
10.721	6.126	22.973	8.944
12.252	7.045	24.504	7.750
13.784	7.903	25.117	7.137

NOTE: ALL DIMENSIONS IN INCHES

101506

Fig. 5 Shaped Hyperflo Parachute Details, Configurations H-4, H-5, H-6, and H-7

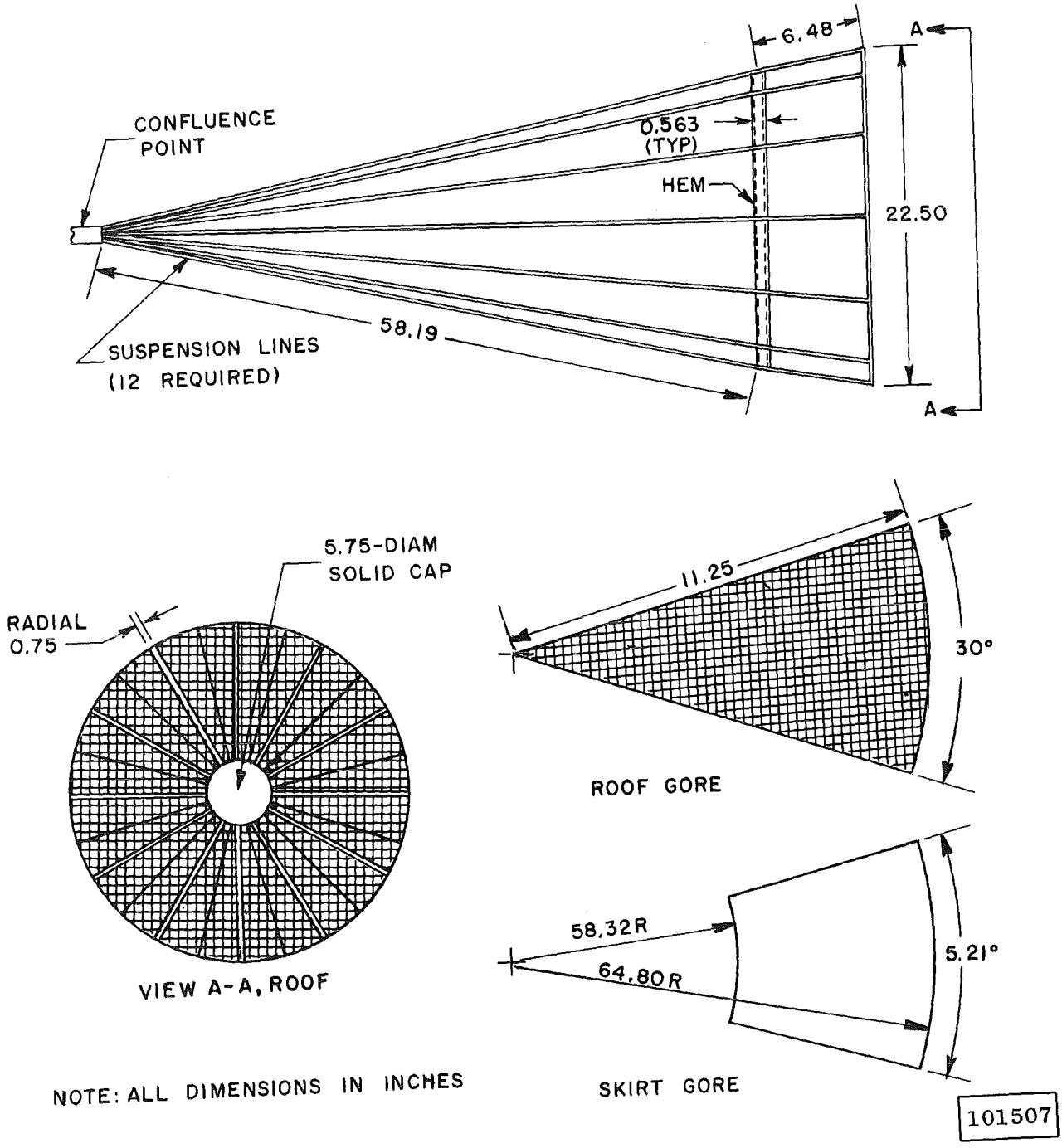

Fig. 6 Hyperflo Parachute Details, Configuration H-8

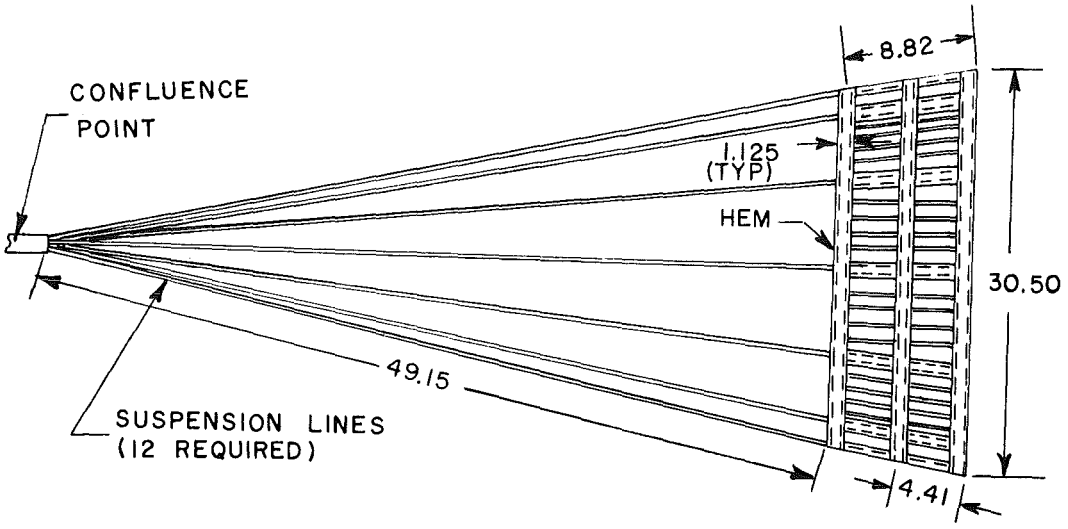

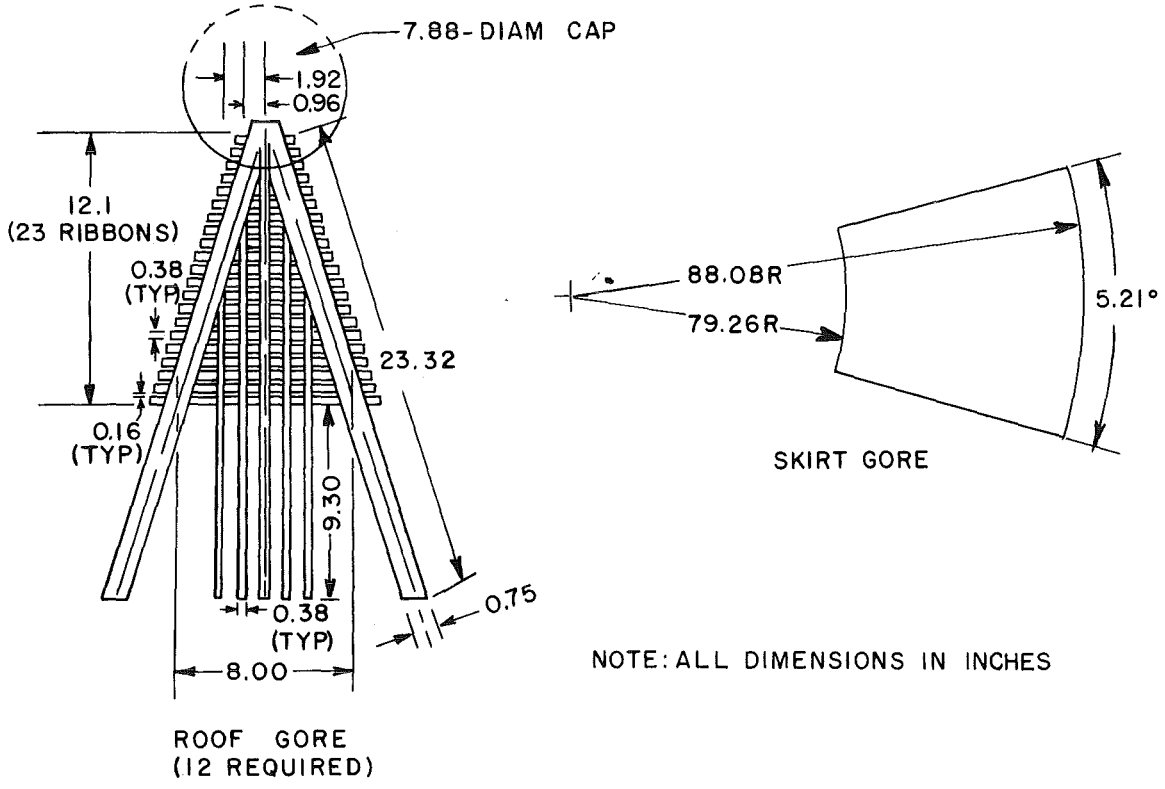

101508

Fig. 7 Hyperflo Parachute Details, Configuration H-9

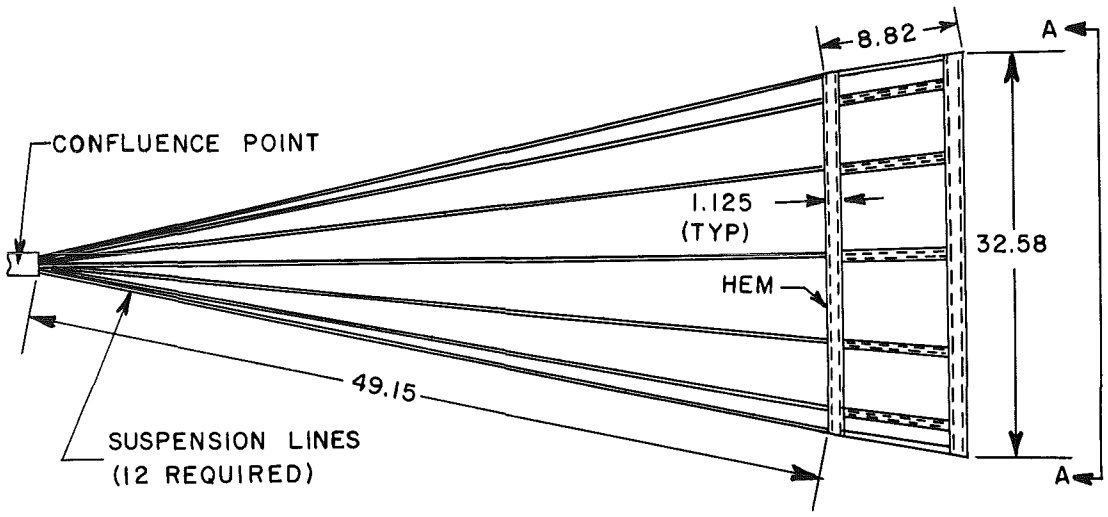

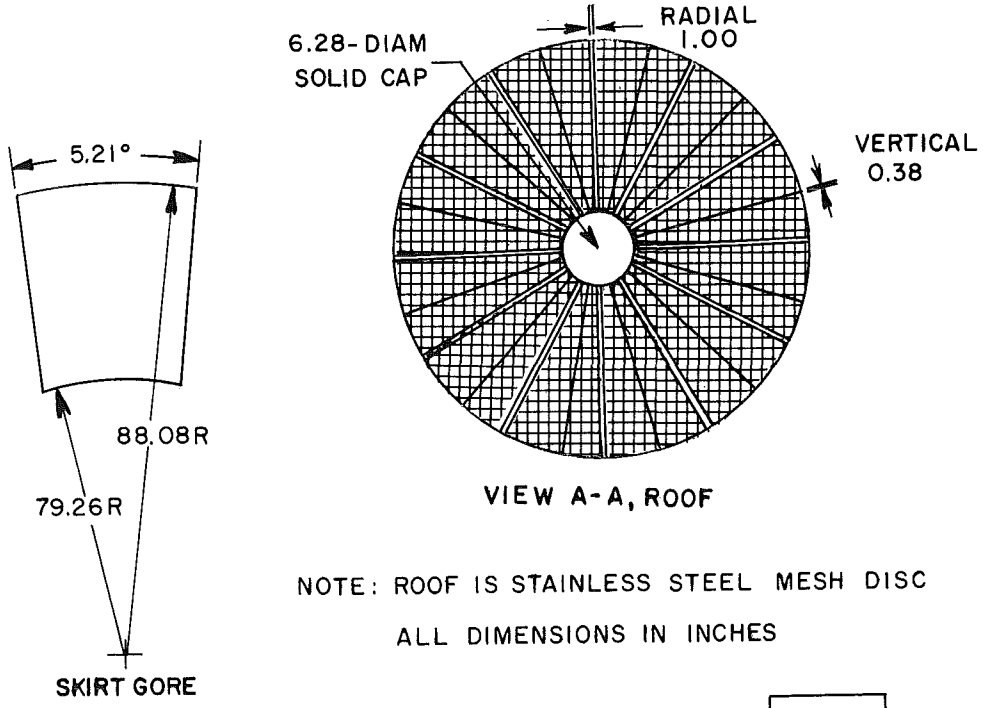

NOTE: ROOF IS STAINLESS STEEL MESH DISC

ALL DIMENSIONS IN INCHES

101509

Fig. 8 Hyperflo Parachute Details, Configuration H-10

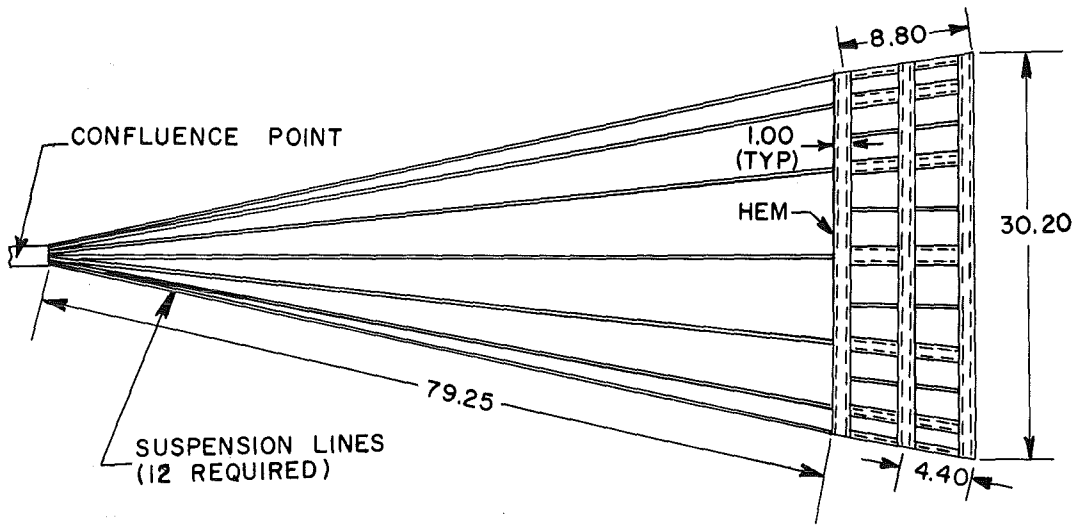

DIMENSIONS IN INCHES

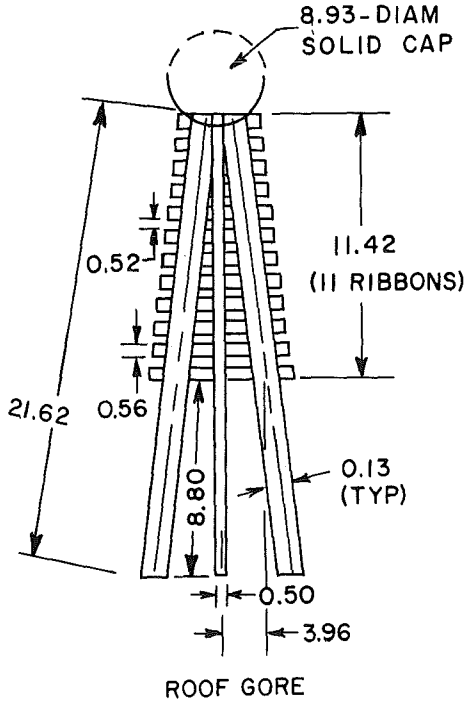

ROOF GORE

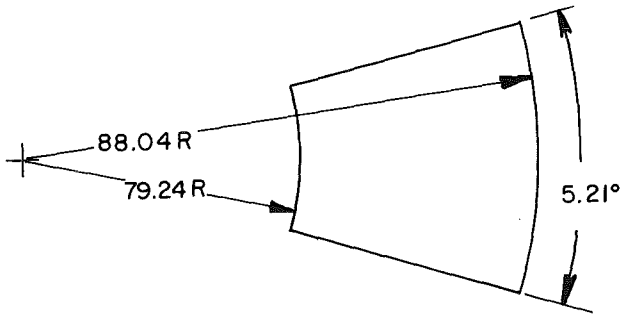

SKIRT GORE

101510

Fig. 9 Hyperflo Parachute Details, Configuration H-11

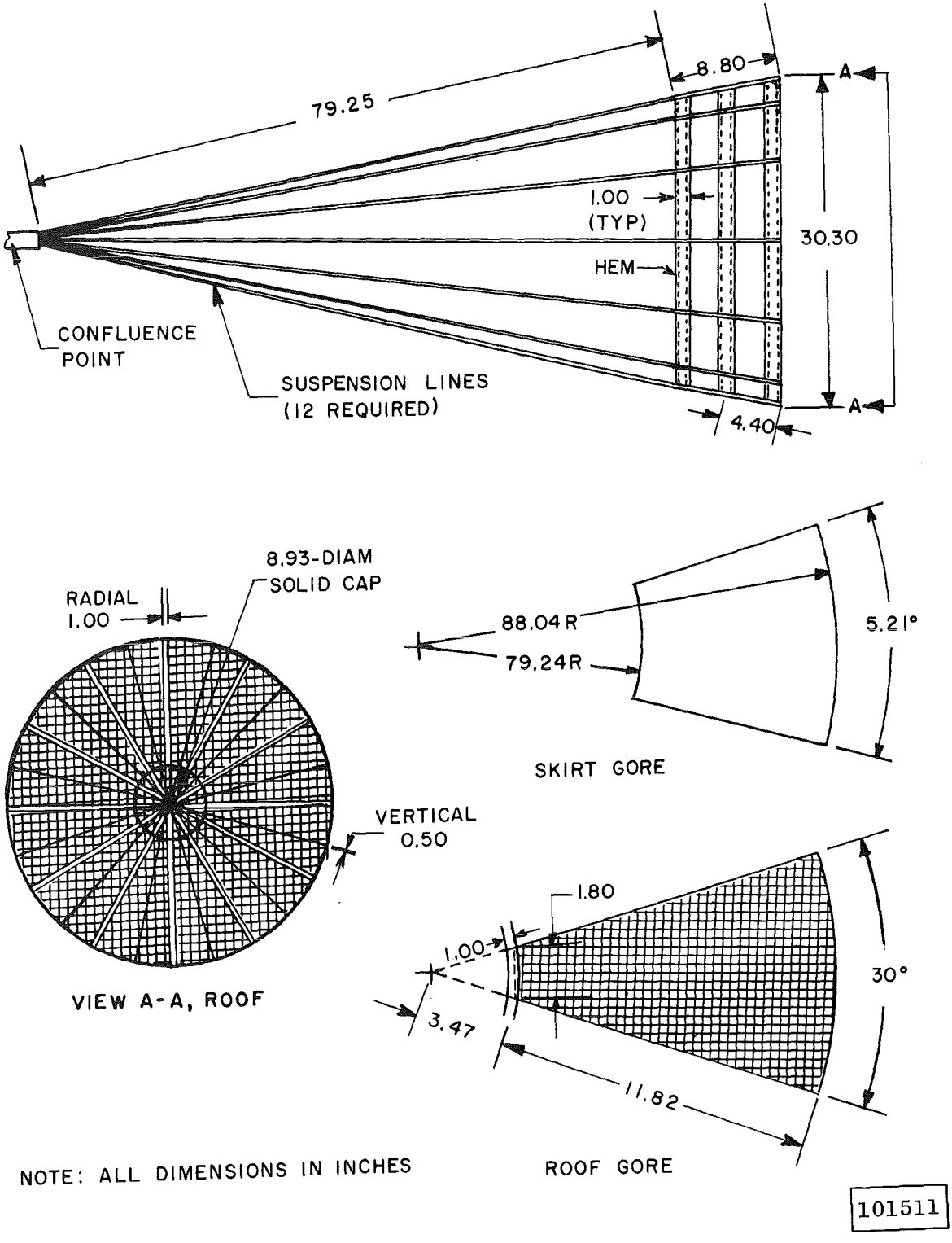

Fig. 10 Hyperflo Parachute Details, Configuration H-12

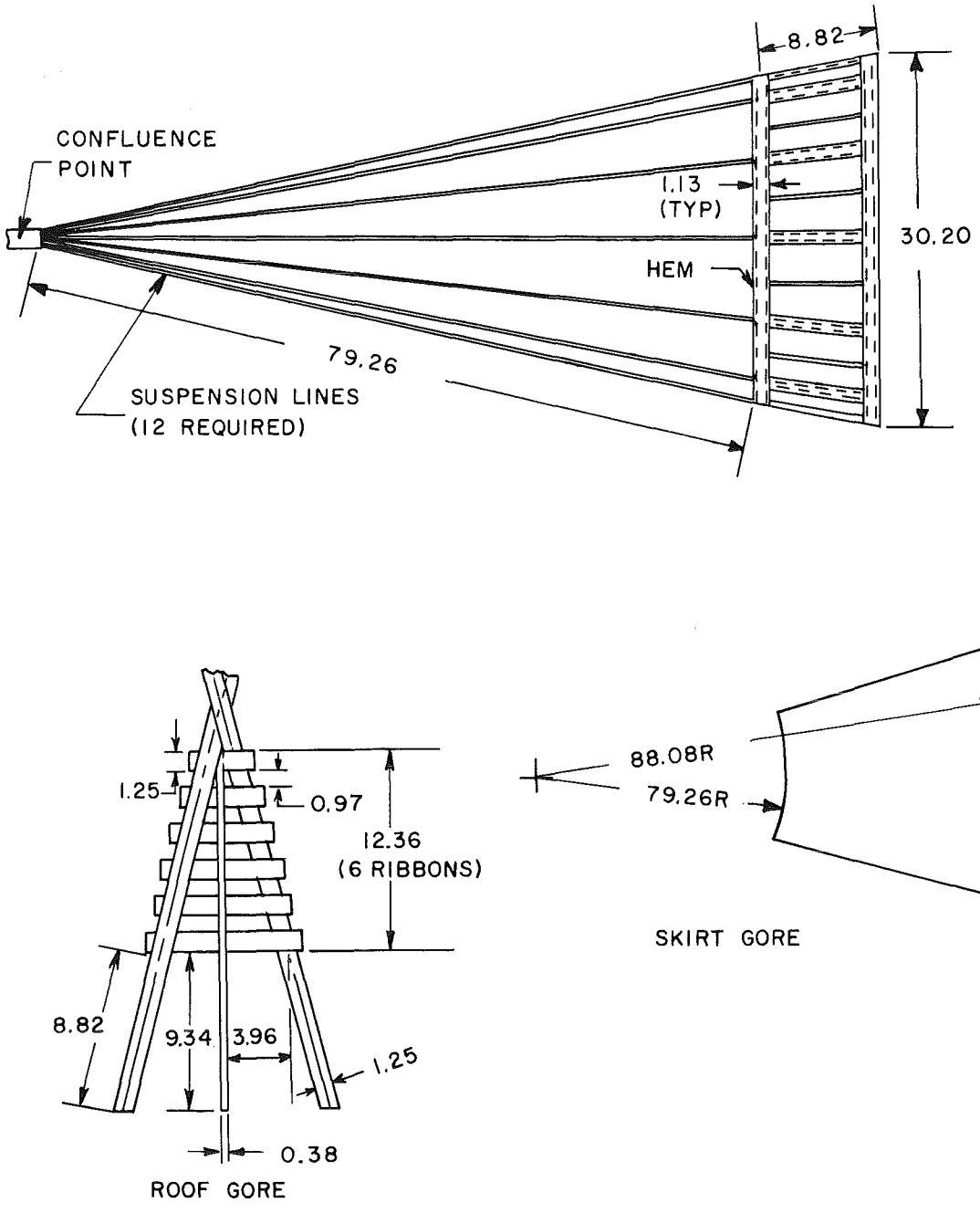

Fig. 11 Hyperflo Parachute Details, Configuration H-13

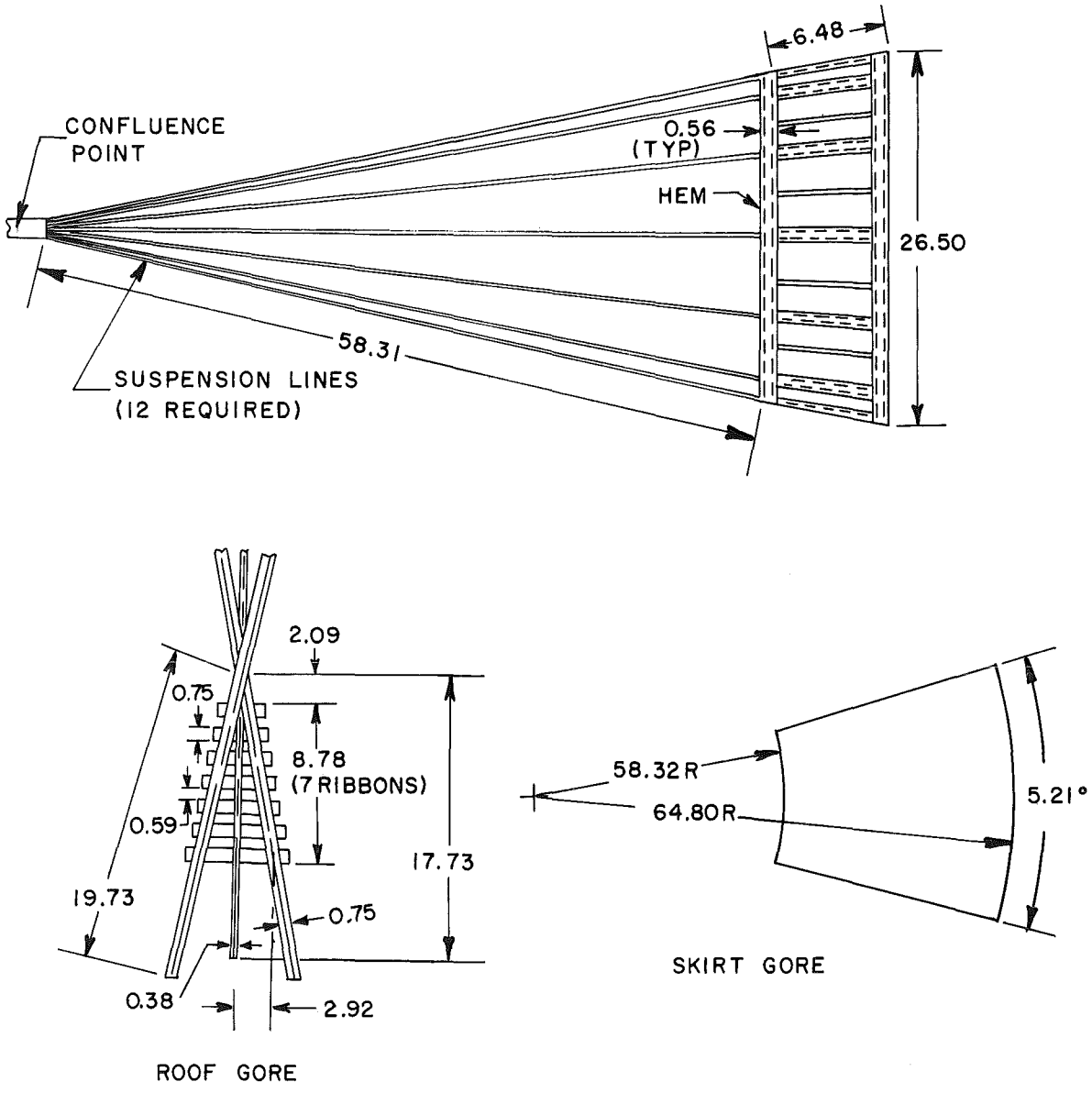

Fig. 12 Hyperflo Parachute Details, Configuration H-14

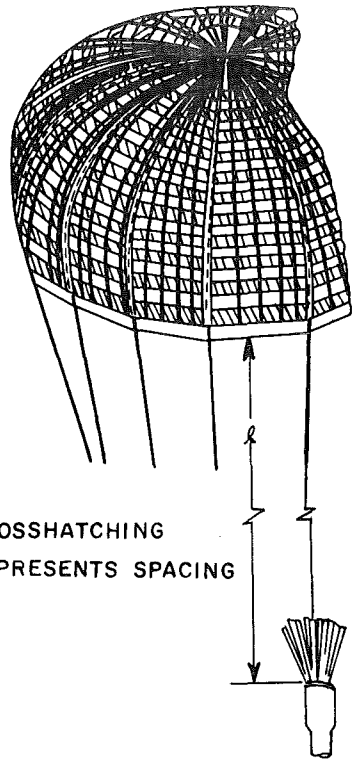

NOTE: CROSSHATCHING REPRESENTS SPACING

CONFIGURATION R-1
HEMISFLO RIBBON
14 GORES
120-IN. NOMINAL DIAMETER
SUSPENSION LINE LENGTH, ℓ = 240 IN.

CONFIGURATION R-2
HEMISFLO RIBBON
14 GORES
120-IN. NOMINAL DIAMETER
SUSPENSION LINE LENGTH, ℓ = 120 IN.

NOTE: ALL DIMENSIONS IN INCHES

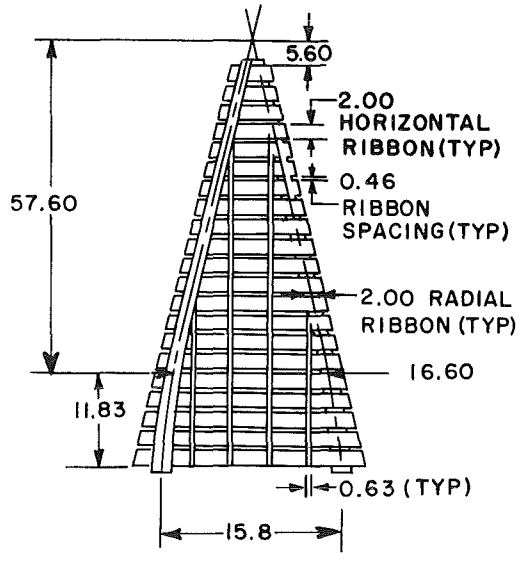

GORE PATTERN
CONFIGURATION R-1

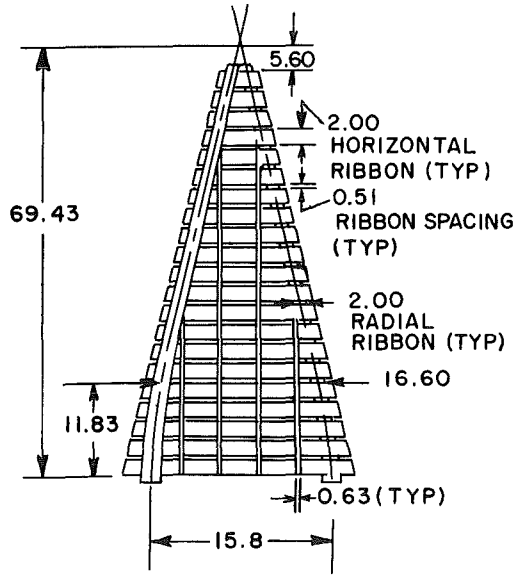

GORE PATTERN
CONFIGURATION R-2

101514

Fig. 13 Hemisflo Parachute Details, Configurations R-1 and R-2

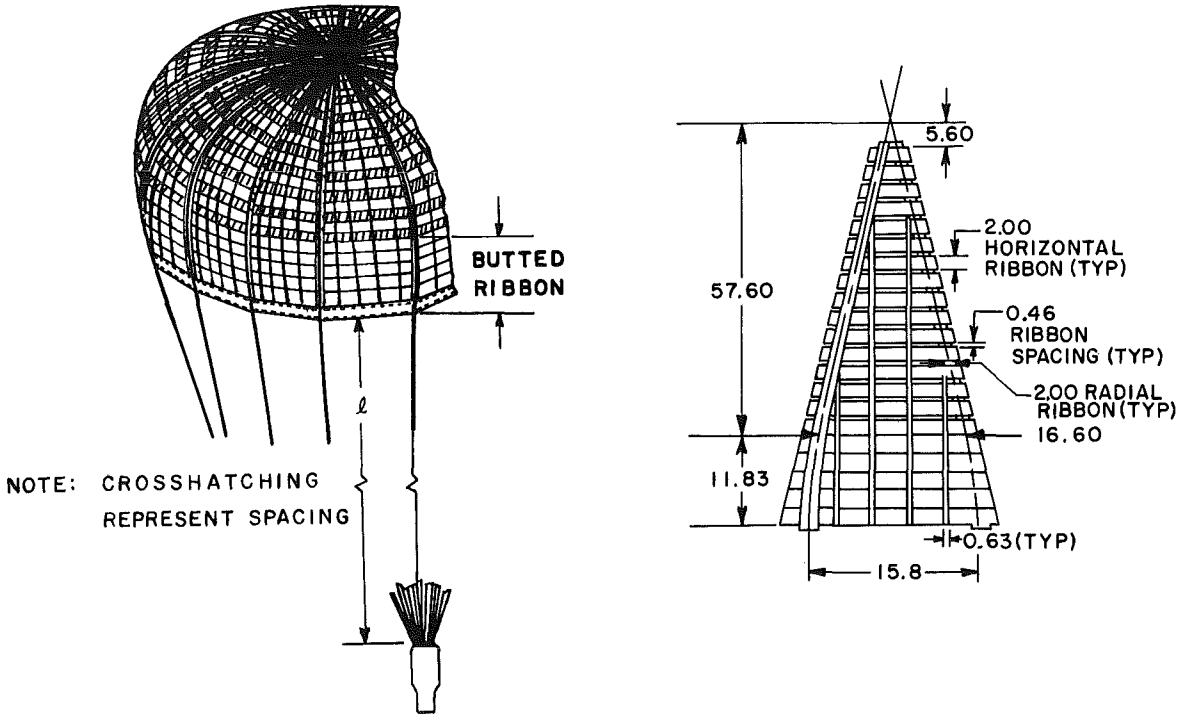

NOTE: ALL DIMENSIONS IN INCHES

CONFIGURATION R-3
HEMISFLO RIBBON
14 GORES
240-IN. NOMINAL DIAMETER
SUSPENSION LINE LENGTH, ℓ = 240 IN.

101515

Fig. 14 Hemisflo Parachute Details, Configuration R-3

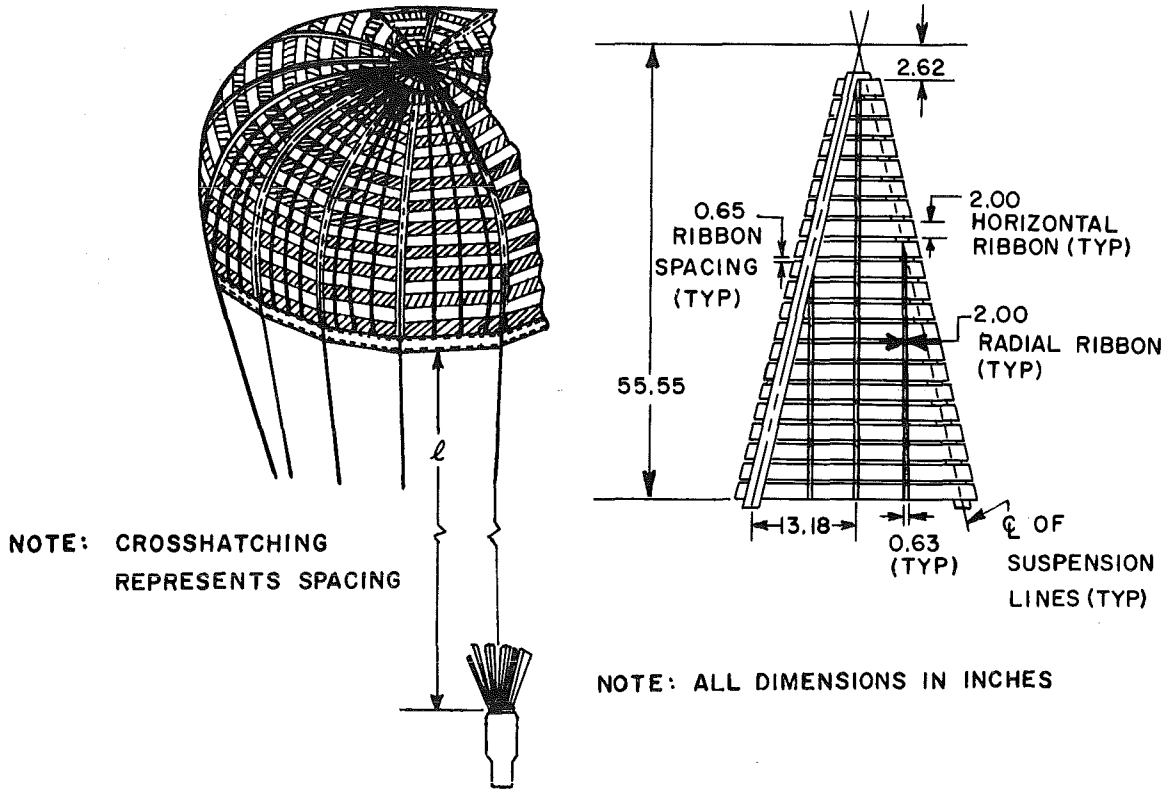

CONFIGURATION R-4
CONICAL RIBBON
14 GORES
120-IN. NOMINAL DIAMETER
SUSPENSION LINE LENGTH,
ℓ = 240 IN.

CONFIGURATION R-5
CONICAL RIBBON
14 GORES
120-IN. NOMINAL DIAMETER
SUSPENSION LINE LENGTH,
ℓ = 120 IN.

101516

Fig. 15 Conical Parachute Details, Configurations R-4 and R-5

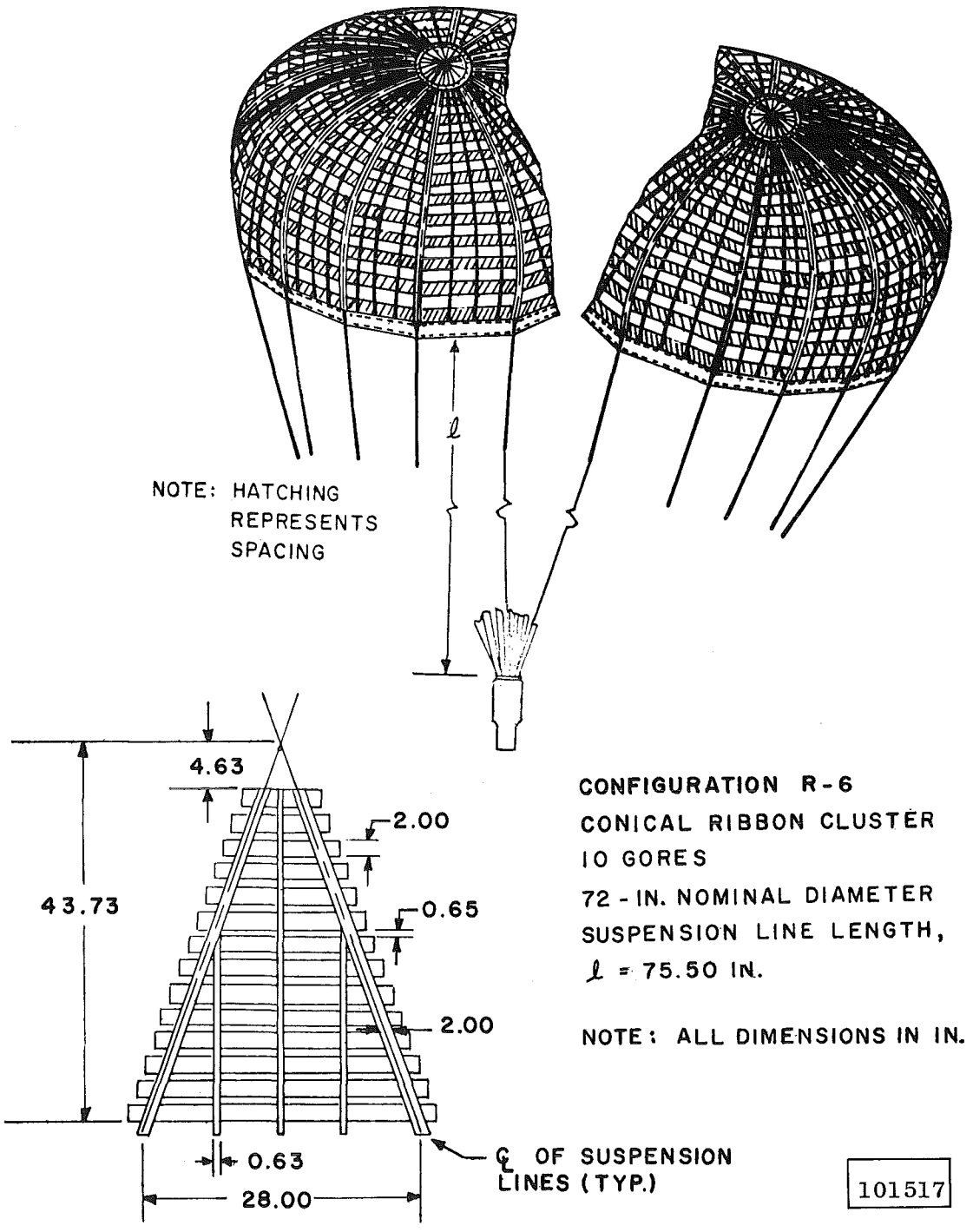

Fig. 16 Conical Parachute Cluster Details, Configuration R-6

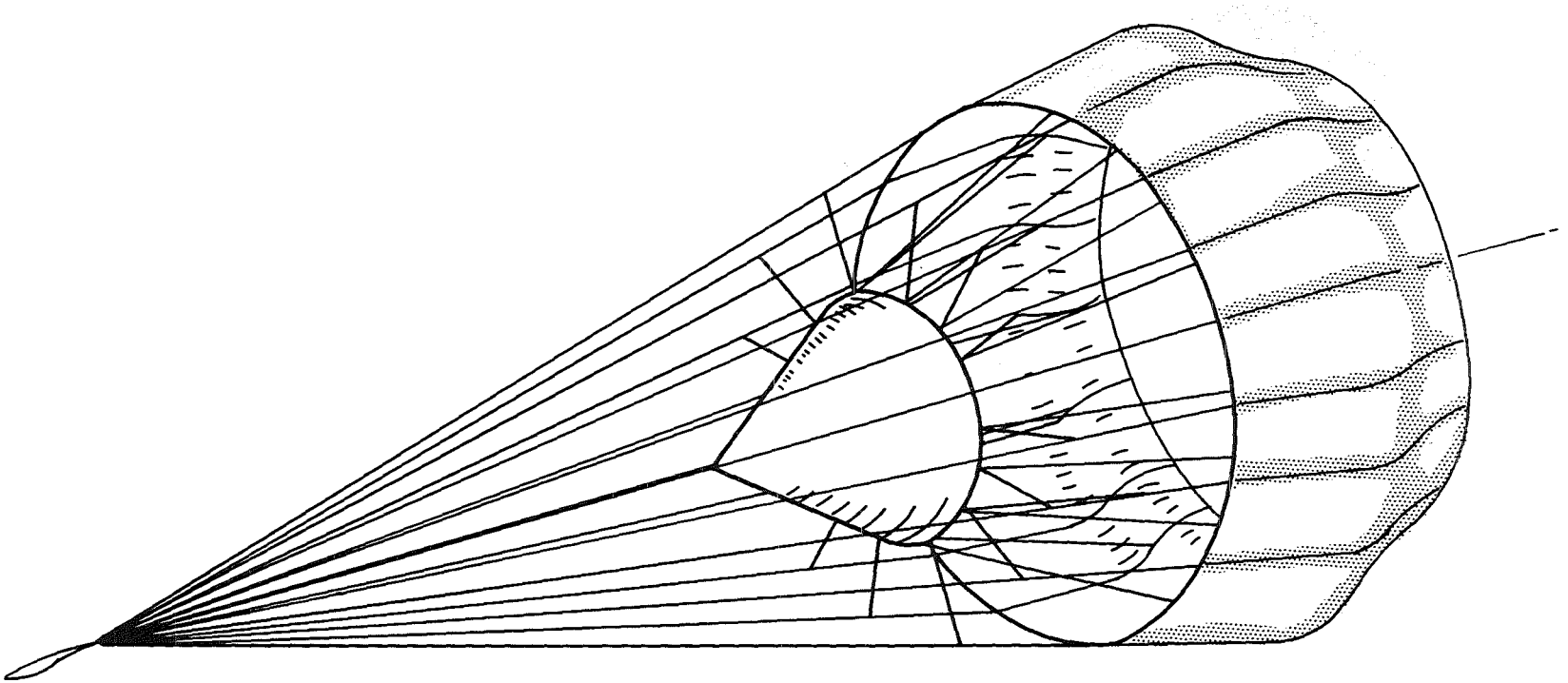

101518

a. Isometric View

Fig. 17 Supersonic-Guide-Surface Parachute, Configuration A-1

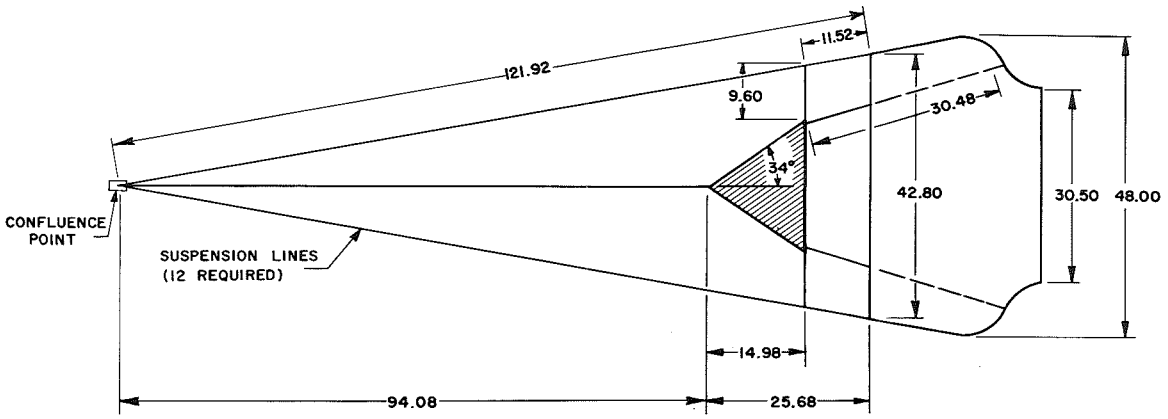

ALL DIMENSIONS IN INCHES

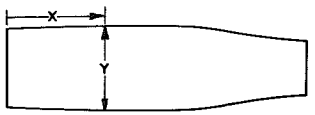

GORE PATTERN

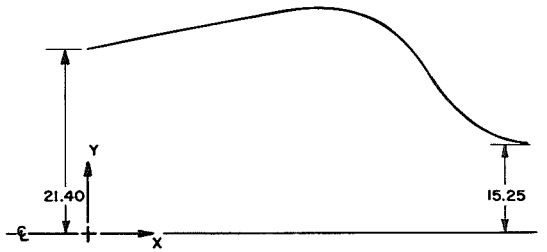

CANOPY PROFILE

X	Y
0	4.20
6.10	4.42
12.19	4.66
13.44	4.70
14.64	4.71
15.84	4.70
17.04	4.68
18.29	4.61
19.58	4.49
21.12	4.30
23.09	3.99
25.30	3.66
27.17	3.39
28.70	3.22
30.10	3.10
31.34	3.03
31.97	3.01

X	Y
0	21.41
6.00	22.51
12.00	23.71
13.20	23.95
14.40	24.00
15.60	23.95
16.80	23.81
18.00	23.47
19.20	22.85
20.40	21.89
21.60	20.35
22.80	18.62
24.00	17.28
25.20	16.42
26.40	15.79
27.60	15.46
28.22	15.36

101519

b. Details

Fig. 17 Concluded

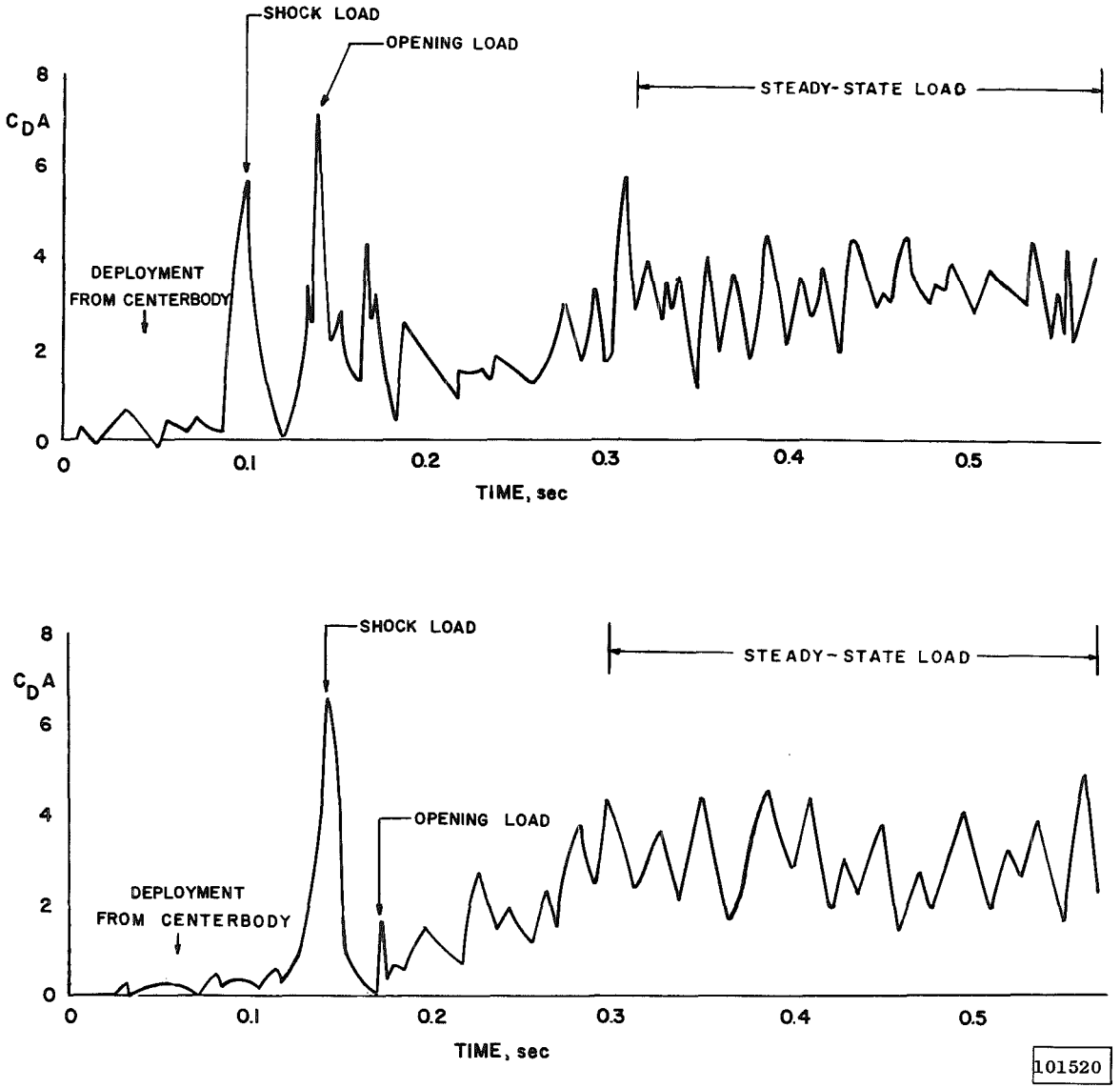

Fig. 18 Typical Parachute Deployment Characteristics

CONFIGURATION	PERCENT POROSITY	CONFIGURATION	PERCENT POROSITY
H-1	13.3	H-8	13.0
H-2	9.4	H-9	7.4
H-3	11.4	H-10	14.5
H-4	15.2	H-11	14.6
H-5	16.9	H-12	14.3
H-6	13.5	H-13	13.7
H-7	9.0	H-14	14.0

NOTE: OPEN SYMBOLS – GOOD INFLATION
CLOSED SYMBOLS – POOR INFLATION

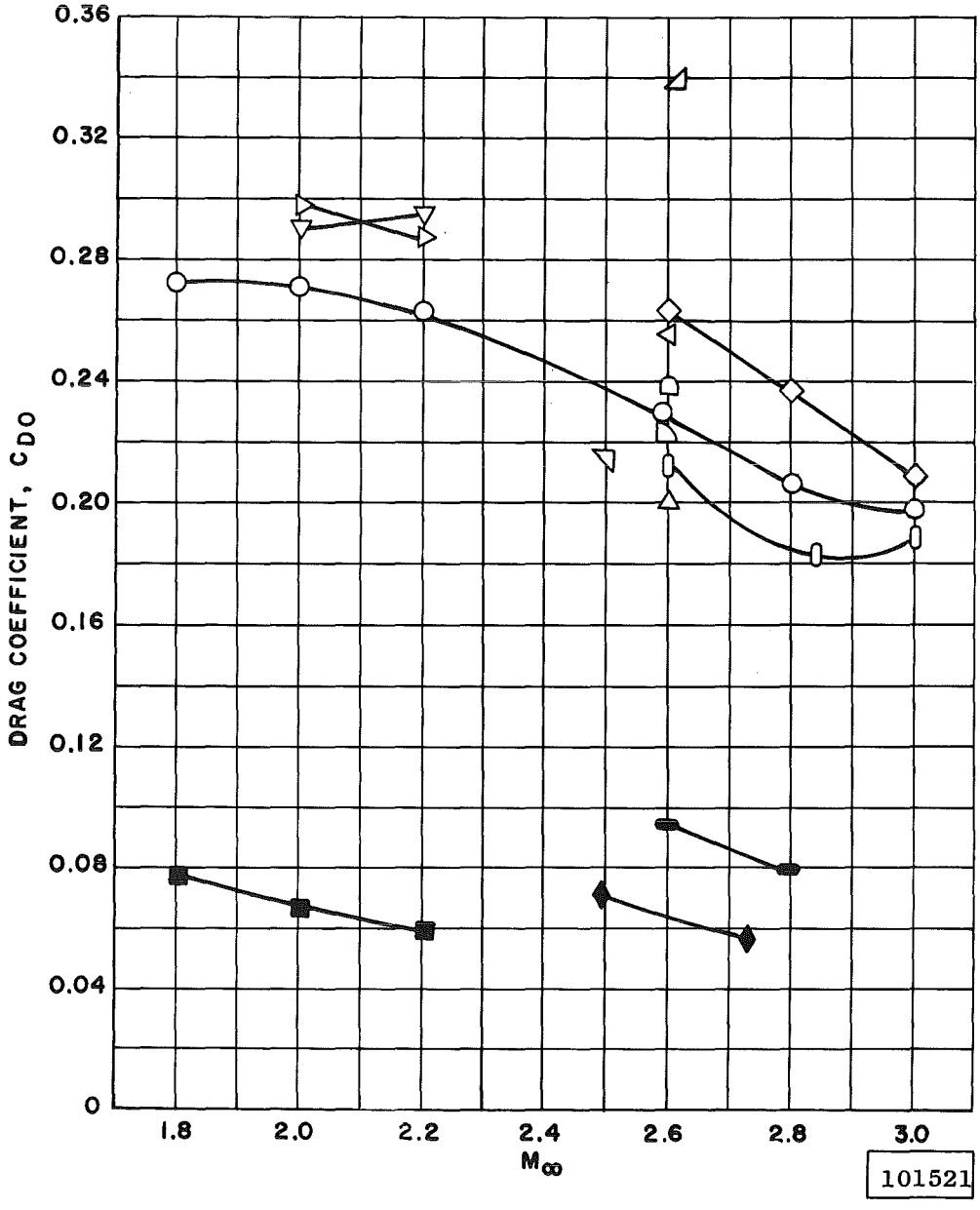

Fig. 19 Variation of Drag Coefficient with Mach Number for Different Hyperflo Parachute Configurations

CONFIGURATION	PERCENT POROSITY	CONFIGURATION	PERCENT POROSITY
H-1	13.8	H-8	13.0
H-2	9.4	H-9	7.4
H-3	11.4	H-10	14.5
H-4	15.2	H-11	14.6
H-5	16.9	H-12	14.3
H-6	13.5	H-13	13.7
H-7	9.0	H-14	14.0

NOTE: OPEN SYMBOLS - GOOD INFLATION
CLOSED SYMBOLS - POOR INFLATION

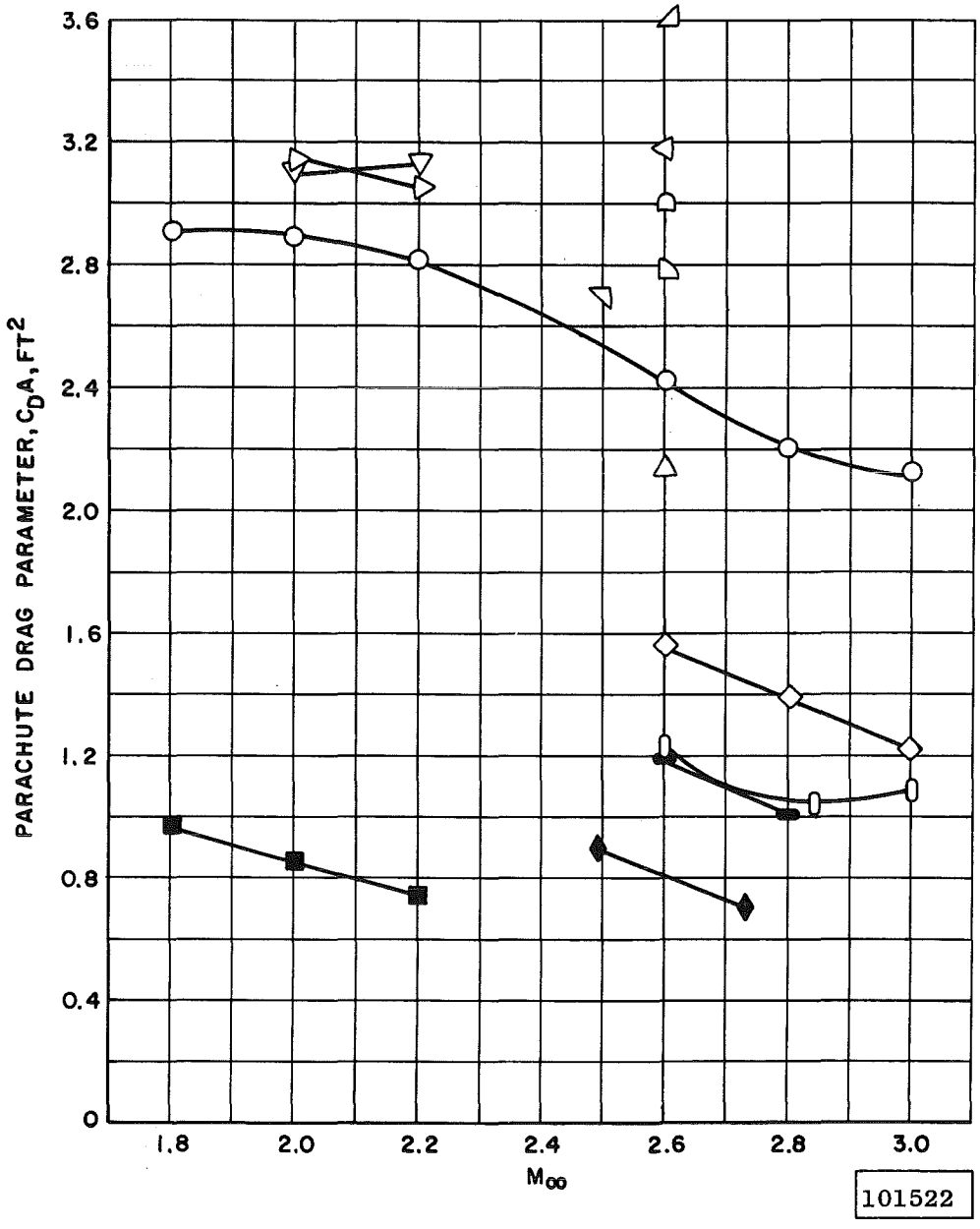

Fig. 20 Variation of the Parachute Drag Parameter with Mach Number for Different Hyperflo Parachute Configurations

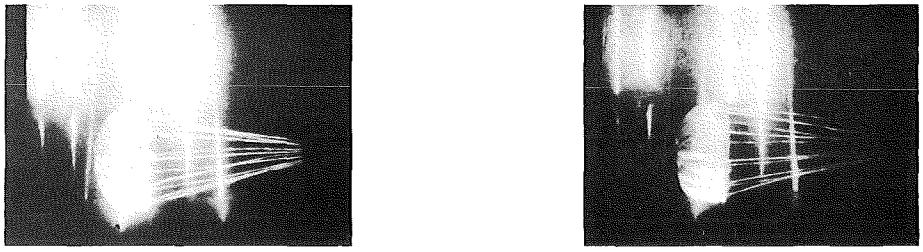

a. Configuration H-3, 11.4% Porosity, $M_\infty = 2.5$

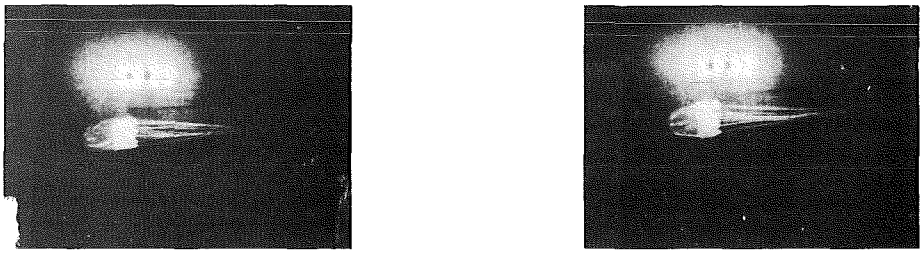

b. Configuration H-4, 15.2% Porosity, $M_\infty = 2.2$

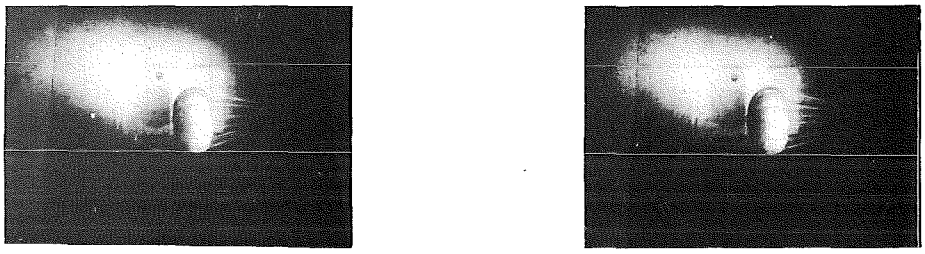

c. Configuration H-7, 9.0% Porosity, $M_\infty = 2.6$

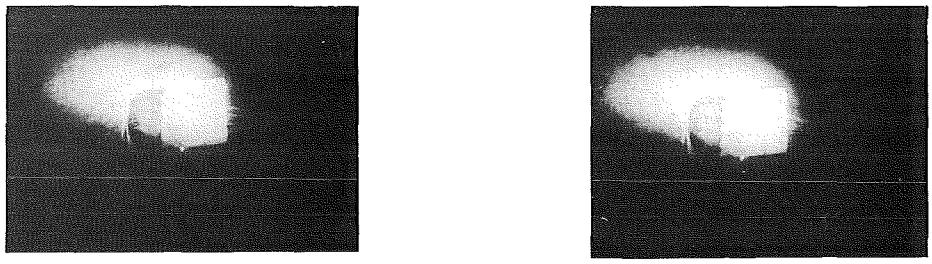

d. Configuration H-9, 7.4% Porosity, $M_\infty = 2.6$

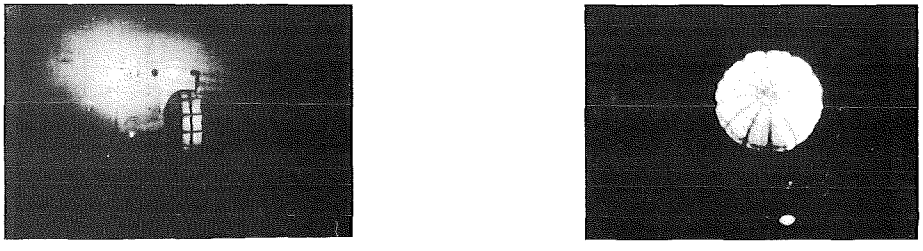

e. Configuration H-12, 14.3% Porosity, $M_\infty = 2.2$

101523

Fig. 21 Photographs of Parachute System during Tests for Various Hyperflo Configurations

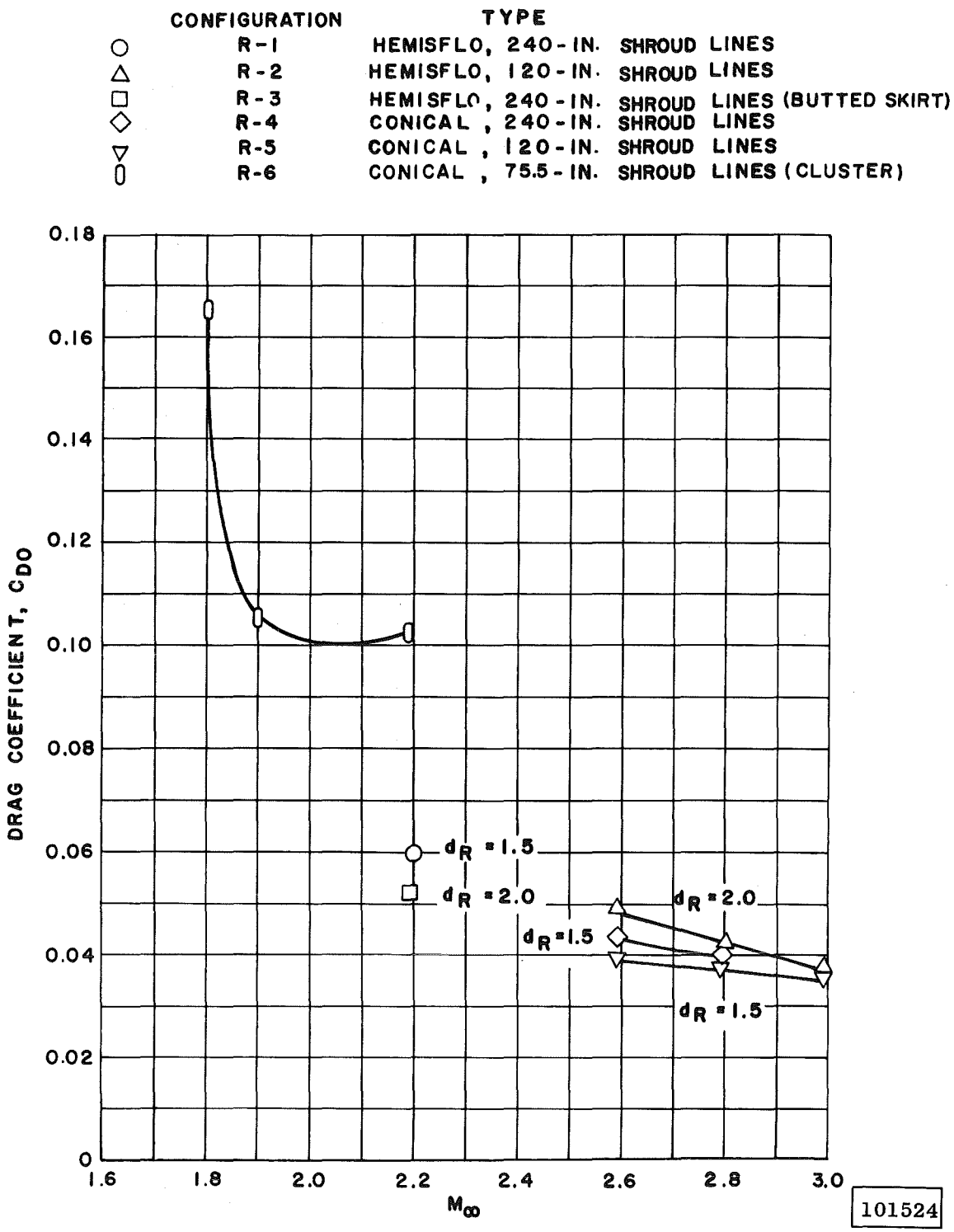

Fig. 22 Variation of Drag Coefficient with Mach Number for Different Hemisflo and Conical Parachute Configurations

CONFIGURATION	TYPE
R-1	HEMISFLO, 240-IN. SHROUD LINES
R-2	HEMISFLO, 120-IN. SHROUD LINES
R-3	HEMISFLO, 240-IN. SHROUD LINES
R-4	CONICAL, 240-IN. SHROUD LINES (BUTTED SKIRT)
R-5	CONICAL, 120-IN. SHROUD LINES
R-6	CONICAL, 75.5-IN. SHROUD LINES (CLUSTER)

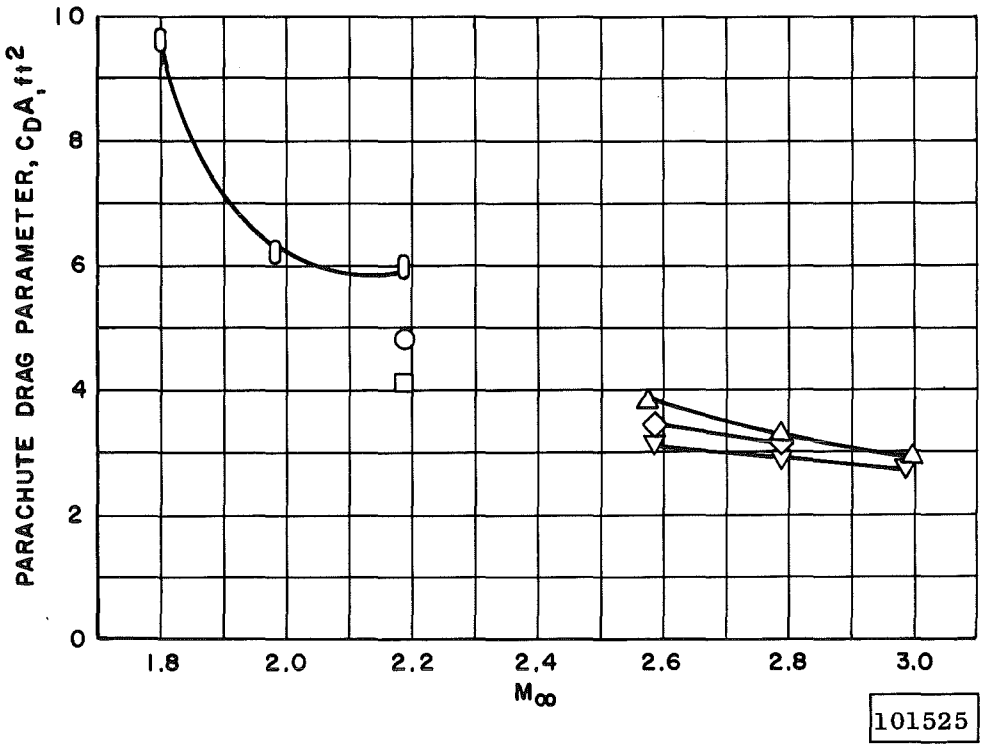

Fig. 23 Variation of the Parachute Drag Parameter with Mach Number for Different Hemisflo and Conical Parachute Configurations

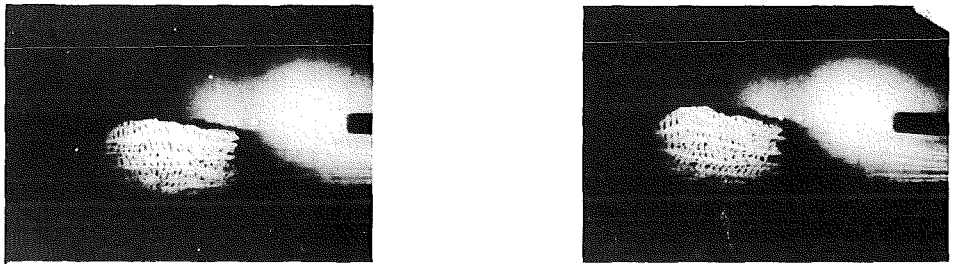

a. Hemisflo Ribbon Parachute, Configuration R-2, $M_\infty = 2.59$

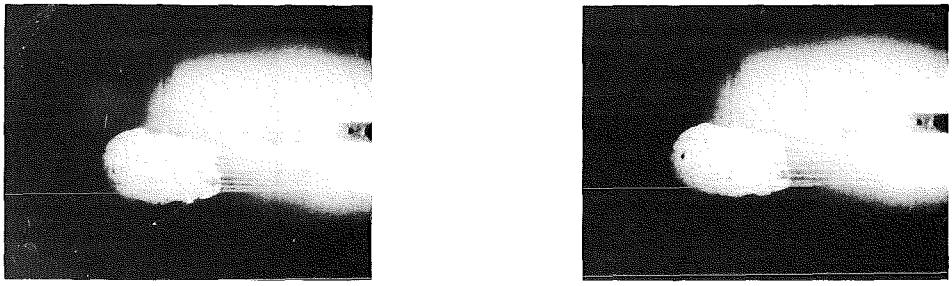

b. Conical Ribbon Parachute, Configuration R-5, $M_\infty = 2.59$

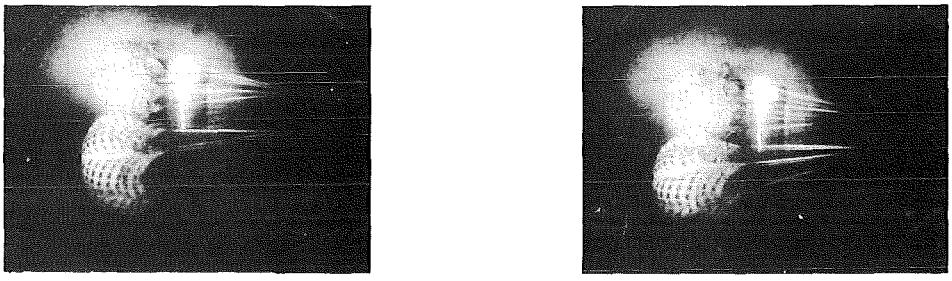

c. Conical Ribbon Parachute Cluster, Configuration R-6, $M_\infty = 1.80$

Fig. 24 Photographs of Parachute System during Tests for Various Hemisflo and Conical Configurations

101526

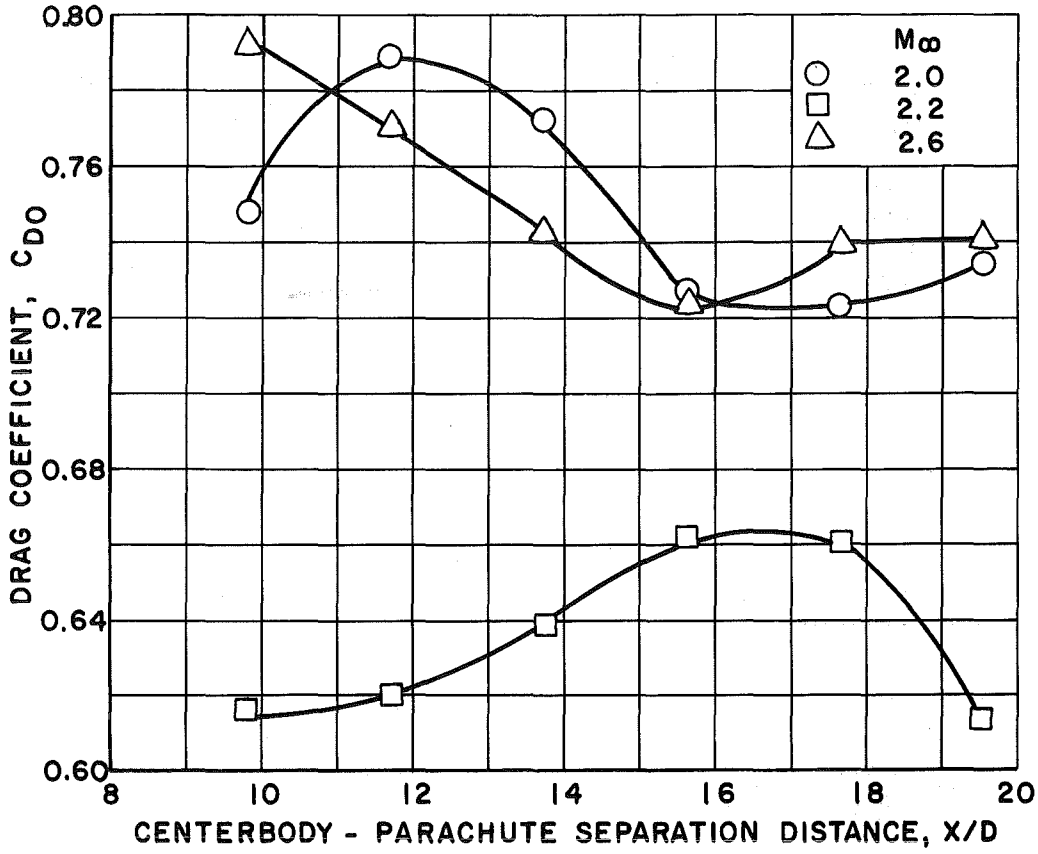

Fig. 25 Variation of Drag Coefficient with Centerbody-Parachute Separation Distance

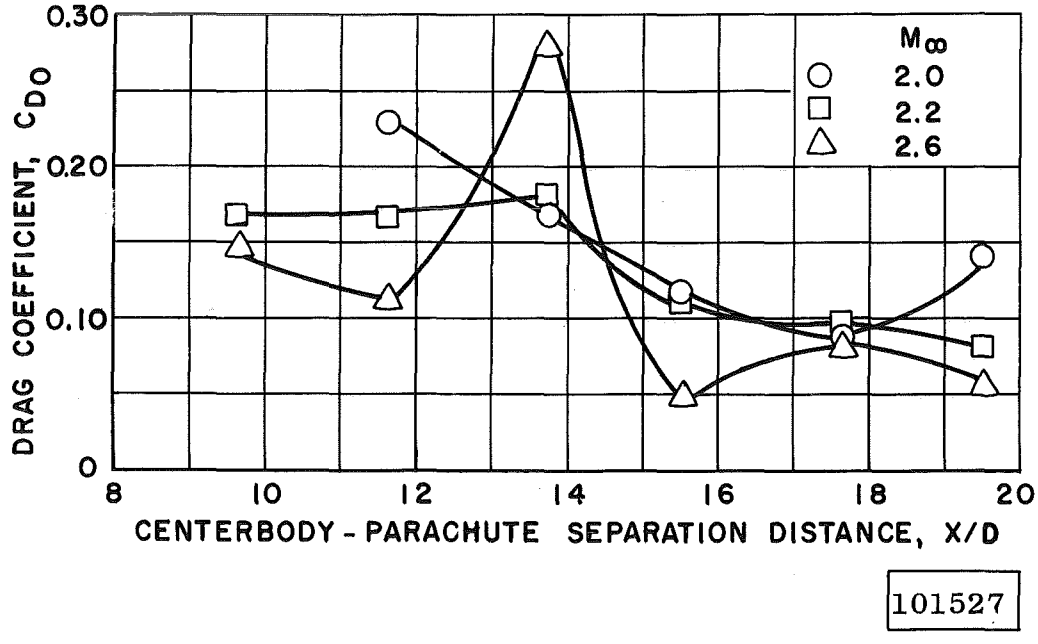

Fig. 26 Peak-to-Peak Drag Coefficient Variation with Centerbody-Parachute Separation Distance

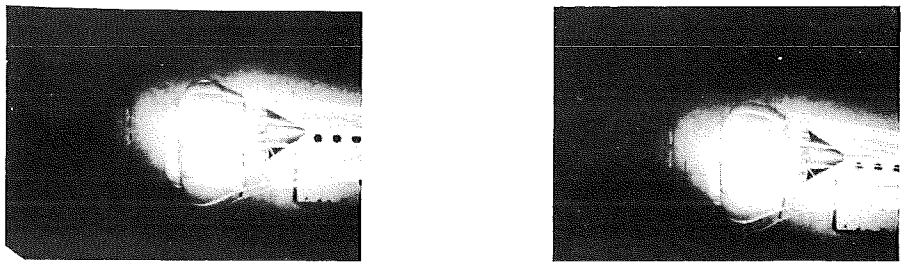

SIDE VIEW

a. Configuration A-1, $M_\infty = 2.6$, X/D = 12

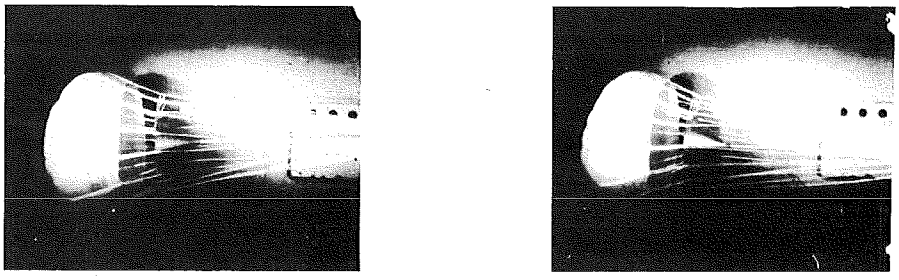

SIDE VIEW

b. Configuration A-1, $M_\infty = 2.6$, X/D = 14

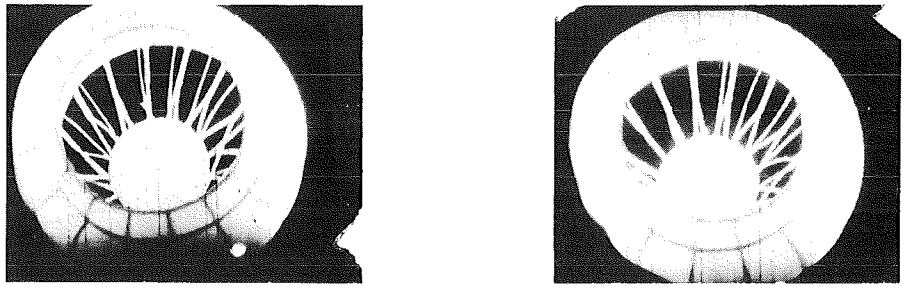

REAR VIEW

c. Configuration A-1, $M_\infty = 2.6$, X/D = 10

Fig. 27 Photographs of Parachute System during Tests for the Supersonic-Guide-Surface Parachute, Configuration A-1

101528